

More on the $O(n)$ model on random maps
 via nested loops:
 loops with bending energy

G. Borot¹, J. Bouttier² and E. Guitter²

¹ Section de Mathématiques

Université de Genève

2-4 rue du Lièvre, Case postale 64, 1211 Genève 4, Suisse

² Institut de Physique Théorique

CEA, IPhT, F-91191 Gif-sur-Yvette, France

CNRS, URA 2306

gaetan.borot@unige.ch

jeremie.bouttier@cea.fr

emmanuel.guitter@cea.fr

Abstract

We continue our investigation of the nested loop approach to the $O(n)$ model on random maps, by extending it to the case where loops may visit faces of arbitrary degree. This allows to express the partition function of the $O(n)$ loop model as a specialization of the multivariate generating function of maps with controlled face degrees, where the face weights are determined by a fixed point condition. We deduce a functional equation for the resolvent of the model, involving some ring generating function describing the immediate vicinity of the loops. When the ring generating function has a single pole, the model is amenable to a full solution. Physically, such situation is realized upon considering loops visiting triangles only and further weighting these loops by some local bending energy. Our model interpolates between the two previously solved cases of triangulations without bending energy and quadrangulations with rigid loops. We analyze the phase diagram of our model in details and derive in particular the location of its non-generic critical points, which are in the universality classes of the dense and dilute $O(n)$ model coupled to 2D quantum gravity. Similar techniques are also used to solve a twisting loop model on quadrangulations where loops are forced to make turns within each visited square. Along the way, we revisit the problem of maps with controlled, possibly unbounded, face degrees and give combinatorial derivations of the one-cut lemma and of the functional equation for the resolvent.

1. Introduction

The study of planar maps, i.e. proper embeddings of graphs in the two-dimensional sphere, has been the subject of an intense activity in combinatorics since the seminal papers of Tutte in the 60's [1]. Recent developments [2] entered the realm of probability theory, by the study of particular ensembles of maps drawn according to some prescribed probability distribution. Such ensembles arise naturally in physics where maps serve as discrete models for various types of fluctuating surfaces such as fluid membranes in soft condensed matter physics or quantum space-times in the theory of two-dimensional quantum gravity. In these contexts, maps have often been equipped with additional degrees of freedom such as spins or particles, giving rise to nice universal critical behaviours in the limit of large maps [3]. A particular important class of such models are the so-called $O(n)$ loop models, where maps carry self- and mutually-avoiding loops, each weighted by n [4-10]. New universality classes are reached in these $O(n)$ loop models when the loops become large and modify the statistics of the underlying map. While the critical exponents have been determined exactly and corroborate the celebrated KPZ relations [11], which relate them to critical exponents of the $O(n)$ model on a fixed regular lattice, little is known on the random geometry of these models.

This has to be contrasted with the case of planar maps without additional degrees of freedom, whose geometry is now well understood. In particular, when maps are endowed with the graph distance, thus are viewed as metric spaces, their generic scaling limit (in the Gromov-Hausdorff sense) is described by a unique remarkable probabilistic object: the Brownian map [2,12,13]. Physically, it corresponds to the universality class of so-called pure gravity. One may escape from this universality class by considering maps with large faces (or “holes”) [14]. More precisely, one works with the so-called Boltzmann ensemble of random maps, where each face receives a weight depending on its degree. If the face degrees are bounded (i.e. the weight for faces of degree k is set to zero for k large enough – which is a usual assumption), the scaling limit is the Brownian map. Non-generic scaling limits may only be obtained by allowing for unbounded degrees, and furthermore fine-tuning the weights in such a way that the degree distribution of a typical face has a heavy tail characterized by an exponent $\alpha \in]1, 2[$. Under this assumption, the scaling limit is a so-called “stable map” of Hausdorff dimension $2\alpha \in]2, 4[$ [14], different from the Brownian map of dimension 4. At first, the fine-tuning of the weights might seem slightly unnatural, but it was proposed that it occurs spontaneously in the context of critical $O(n)$ loop models on random maps: considering a sample configuration of such a model, if one erases all the outermost loops and their contents, the resulting map (called *gasket*) is a map drawn according to a Boltzmann ensemble with non-generic scaling limit.

This mechanism was investigated in a recent paper [15], for a particular class of $O(n)$ loop models on tetravalent maps (dual to quadrangulations). Notably, n was shown to be generically related to α via $n = 2 \sin \pi \alpha$ (where n should vary between 0 and 2 in order for the loop model to have critical points, the two corresponding possible values of α being associated respectively with the dense and dilute universality classes). A full explicit solution of the model was obtained for a specific model, the so-called

rigid loop model where loops are forced to go straight within each visited square. The purpose of the present paper is to extend the study of [15] to the largest possible class of $O(n)$ loop models amenable to a full solution by the same techniques. As we shall discover, this class corresponds to models with loops visiting triangles only, and with an additional *bending energy* term which controls the rigidity of the loops. These models interpolate, upon varying the bending energy, between the standard $O(n)$ loop model on triangulations [4-10] and the rigid loop model of [15] on quadrangulations (with squares formed of two triangles). Note that here, we define our model only on planar maps. Extending and solving it for maps of arbitrary topology would present no difficulty, following the lines of [16], although we do not address it here. Indeed, once the planar case is solved, the answer for other topologies should be given by a topological recursion formula.

The paper is organized as follows: in Section 2, we recall the nested loop approach initiated in [15] as a general strategy that allows to reformulate any $O(n)$ loop model as a model of maps with controlled face degrees. In practice, the nested loop approach consists of a gasket decomposition (Section 2.1) obtained by cutting the maps along the superimposed loops, resulting in a bijective coding of the $O(n)$ loop configurations. This coding translates into a *fixed point condition* for the degree-dependent weights in the equivalent problem of maps with controlled face degrees (Section 2.2). This in turn translates into a *functional equation* for the so-called *resolvent* of the $O(n)$ loop model, which is the generating function for loop configurations on maps with a boundary of controlled length (Section 2.3). Here, in contrast with [15], we use a shortcut to directly write down the functional equation from the fixed point condition. Explicit examples of functional equations are given in Section 2.4 for a number specific models that have been considered before. In all generality, the functional equation involves a bivariate ring generating function which is the (grand canonical) generating function for the immediate surroundings of the loops. Section 3 is devoted to finding the largest possible class of models for which the functional equation may be solved by a straightforward generalization of the techniques presented in [15] and originally developed by Kostov [5], Kostov and Staudacher [6], Eynard and Zinn-Justin [7] and Eynard and Kristjansen [8,9], and reformulated later in terms of algebraic geometry [16]. These models correspond to having a bivariate ring generating function with a single pole, as explained in Section 3.1, in which case the functional equation simplifies drastically and involves crucially some (general) decreasing homographic involution. Interestingly enough, all these models may be realized by considering a model of loops visiting triangles only and weighted by some particular *bending energy*, as explained in Section 3.2. The details of the solving technique are finally recalled in Section 3.3. This strategy is applied explicitly in Section 4 to study the phase diagram of the $O(n)$ loop model with bending energy defined on triangulations, i.e. when the unvisited faces are themselves triangles. An explicit derivation of the non-generic critical line, corresponding to the location in the parameters of the model of its dense and dilute phases, is given in Section 4.1 while the whole phase diagram is discussed in Section 4.2. The limit $n \rightarrow 0$ of the model is discussed in Section 4.3 as a number a combinatorial simplifications arise in this case.

Section 5 is devoted to the solution by similar techniques of the so-called *twisting loop* model on quadrangulations which is yet another particular case of the model considered in [15] where, in contrast with the rigid loop model, loops are forced to make a turn inside each visited square. Our derivation of the functional equation for the resolvent of the $O(n)$ model relies on the analytic properties of the similar resolvent in a model of maps with controlled face degrees. We review these properties in Section 6. We present in Section 6.1 a new combinatorial proof of the so-called *one-cut lemma* and rederive in Section 6.2 the functional equation satisfied by the resolvent. Section 6.3 is devoted to the proof of a technical result while the case of complex-valued face weights is briefly discussed in Section 6.4. We gather our conclusions in Section 7.

2. The nested loop approach

2.1. The gasket decomposition

In this paper, we consider loop configurations on planar maps defined as follows: given a map, a *loop* is an undirected simple closed path on the dual map (i.e. it visits edges and vertices of the dual map, hence visits faces and crosses edges of the original map). A *loop configuration* is a set of disjoint loops. Choosing a loop configuration amounts to choosing a set of crossed edges in such a way that each face is incident to exactly 0 or 2 crossed edges (with multiplicities, to account for self-folded faces). We call *map with a boundary of length p* ($p \geq 1$) a rooted planar map where the *external* face (i.e. the face on the right of the root edge) has degree p . By convention, when considering loop configurations on maps with a boundary, we demand that the external face is not visited by a loop. The external face allows to distinguish the exterior and interior of a loop. In particular, we may associate to each loop its *outer* (resp. *inner*) *contour* consisting of all the exterior (resp. interior) edges that are incident to a face visited by the loop. Each contour is a closed, but non-necessarily simple, path on the map.

Following [15], let us define the *gasket decomposition* of a map with a boundary of length p endowed with a loop configuration. It consists in cutting the map along the outer and inner contours of each *outermost* loop. This splits the map into several connected components, which are as follows.

- The *gasket* is the map spanned by the edges which were exterior to all the loops.
- Each outermost loop yields two connected components:
 - its *ring* is formed by the faces visited by the loop,
 - its *internal map* is the map spanned by the edges which were interior to the loop. This map is endowed with a loop configuration consisting of all the loops which were originally interior to the outermost loop at hand.

All these components are rooted canonically, as displayed in Fig. 1. Thus, each internal map may be viewed as a map with a boundary of the same nature as the original map.

By construction, the gasket is itself a map with a boundary of length p (note that the gasket contains all the edges incident to the external face), without loops, and whose inner faces are of two types: *regular* faces corresponding to faces of the original map

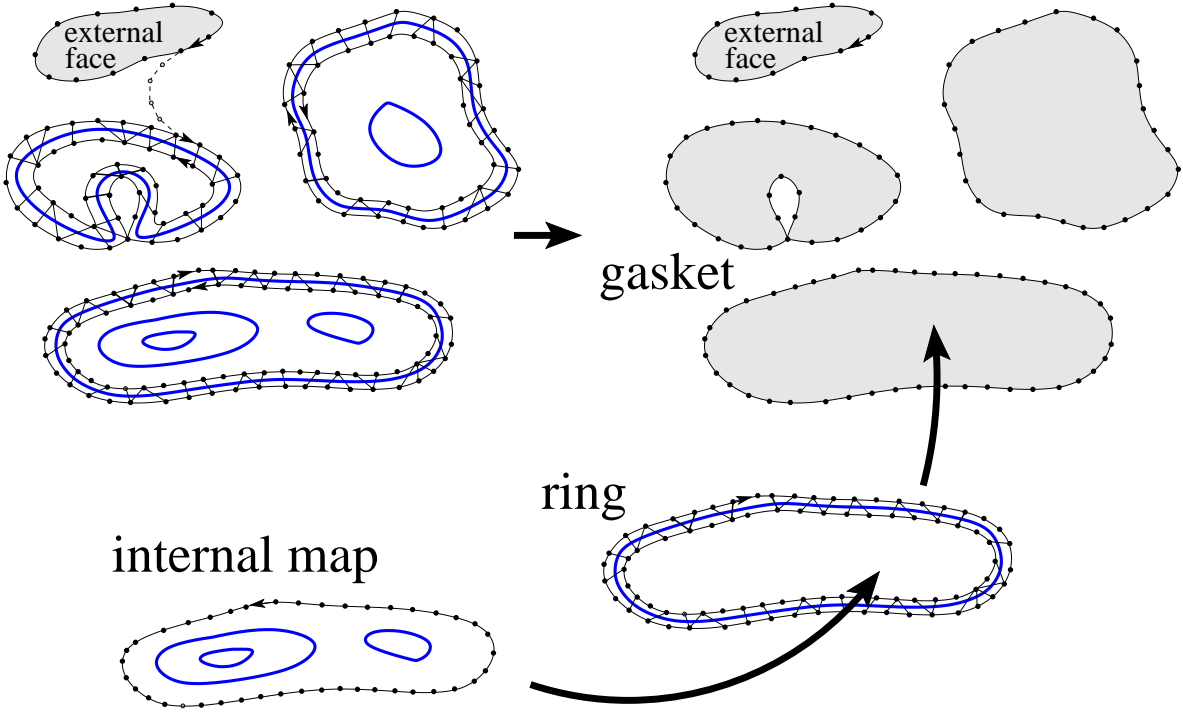


Fig. 1: A schematic picture of the gasket decomposition. Cutting the map along the outer contour of each outermost loop and removing the interior of these outer contours yields the gasket, with a new type of faces: the holes. Upon cutting along the inner contours of the same loops, the former content of each hole may itself be divided into a ring and an internal map. All these components are rooted by some canonical (yet irrelevant) procedure. We may for instance consider the leftmost loop-avoiding shortest path from the root edge of the map (i.e. the root of the external face) to the outer contour of any outermost loop. This selects an edge on this contour which can be used as root for the corresponding ring. By then transferring the root from the outer to the inner contour by some local rule, it gives a root for the corresponding internal map.

that were exterior to all the loops, and *holes* delimited by the outer contours of the former outermost loops. Note that an outermost loop having outer and inner contours of respective lengths k and k' gives rise to a hole of degree k in the gasket and to an internal map with a boundary of length k' . Furthermore, both the gasket and internal map may contain separating vertices. In particular, a multiple point along the outer (resp. inner) contour yields a separating vertex incident to a hole in the gasket (resp. to the external face of the internal map). By contrast, we decide that multiple points on the contours are split into distinct vertices in the ring, so that both sides of the ring are simple paths of lengths k and k' .

To summarize, the gasket decomposition provides a bijection between, on the one hand, maps with a boundary of length p endowed with a loop configuration, and on the other hand, maps with a boundary of length p with regular faces and holes, where

each hole of degree k ($k \geq 1$) is endowed with (i) a ring with sides of lengths k and k' for some $k' \geq 0$ and (ii) a map with a boundary of length k' endowed with a loop configuration (by convention there is a unique map with a boundary of length 0, the vertex-map, with no loops).

2.2. The fixed-point condition

We may use the above gasket decomposition to relate the partition function of various loop models on random maps to the multivariate generating function for maps with prescribed face degrees. More precisely, consider an $O(n)$ loop model on maps with a boundary where the Boltzmann weight of a configuration (i.e. a map endowed with a loop configuration) is the product of:

- for each $k \geq 1$, a weight $g_k^{(0)}$ per inner face of degree k not visited by a loop,
- a weight per loop that *only depends on the structure of its ring*, that we write in the form $n w_r$ where n is the loop fugacity and w_r is, at this stage, an arbitrary function of the ring r . In all the cases discussed in this paper, w_r will be given as a product of some local weights, leaving n as the only non-local weight in the model.

Let us denote by F_p the partition function for such an $O(n)$ loop model on maps with a boundary of length p , which depends on n , the $g_k^{(0)}$'s and the w_r 's (by convention, we set $F_0 = 1$). It follows from the gasket decomposition that F_p is obtained by specializing a multivariate generating function for maps without loops but with controlled face degrees. More precisely, we denote by $\mathcal{F}_p(g_1, g_2, \dots)$ the multivariate generating function for maps with a boundary of length p with weight g_k per inner face of degree k (by convention $\mathcal{F}_0 = 1$), and we introduce the *ring generating function*

$$A_{k,k'} = \sum_{r \in \mathcal{R}(k,k')} w_r \quad (2.1)$$

where $\mathcal{R}(k, k')$ is the set of rings with outer length k and inner length k' , rooted on the outer contour. Then, the gasket decomposition translates into the relation

$$F_p = \mathcal{F}_p(g_1, g_2, \dots) \quad (2.2)$$

at values of the weights g_k satisfying the *fixed-point condition*

$$g_k = g_k^{(0)} + n \sum_{k' \geq 0} A_{k,k'} \mathcal{F}_{k'}(g_1, g_2, \dots) \quad \text{for all } k \geq 1. \quad (2.3)$$

Let us now give a few examples of ring generating functions. If we assume that the loops only visit triangles, and that the weight for a ring r made of m triangles is $w_r = h^m$, then we recover the $O(n)$ loop model studied in [5-9]. We have

$$A_{k,k'}^{\text{tri}} = \binom{k+k'-1}{k'} h^{k+k'}, \quad (2.4)$$

as seen by the following simple counting argument: a ring with outer length k and inner length k' is a sequence of $k + k'$ triangles, k of which are facing outwards, that we may read starting from the distinguished outward-facing triangle carrying the root of the ring.

Consider now the $O(n)$ loop model studied in [15]. Here, the loops only visit squares, and there are two types of visited squares: those such that the loop crosses opposite sides (type b) and those such that the loop crosses adjacent sides (type c). The weight for a ring r made of m squares of type b and m' squares of type c is $w_r = h_1^m h_2^{m'}$, and the ring generating function is given by [15, eq. (2.4)]

$$A_{k,k'}^{\text{quad}} = \sum_{j=0}^{\min(k,k')} \frac{2k}{k+k'} \frac{(k+k')!}{(2j)!(k-j)!(k'-j)!} h_1^{2j} h_2^{k+k'-2j} . \quad (2.5)$$

In particular, for $h_2 = 0$ we recover the so-called *rigid loop* model for which

$$A_{k,k'}^{\text{rigid}} = \delta_{k,k'} h_1^k \quad (2.6)$$

as seen directly by noting that the unique ring of outer length k is made of k squares and has inner length $k' = k$. Alternatively, let us consider the opposite case $h_1 = 0$ that we call the *twisting loop* model. Clearly, the associated ring generating function $A_{k,k'}^{\text{twist}}$ vanishes whenever k or k' is odd, and

$$A_{2k,2k'}^{\text{twist}} = 2 \binom{k+k'-1}{k'} h_2^{k+k'} , \quad (2.7)$$

as seen directly by a counting argument similar to that for (2.4) (there are 2 possible choices for the position of the root on its incident outward-facing square, thus the extra factor 2).

In general, we may encode the $A_{k,k'}$'s into the grand generating function

$$A(x, y) = \sum_{k \geq 1} \sum_{k' \geq 0} A_{k,k'} x^k y^{k'} . \quad (2.8)$$

The apparent asymmetry between k and k' in the above expressions is related to the fact that the ring has a distinguished edge on the outer contour. Assuming that the ring weight does not depend on the position of the distinguished edge, we may write

$$A(x, y) = x \frac{\partial}{\partial x} \log H(x, y) \quad (2.9)$$

where $\log H(x, y)$ is now the generating function for unrooted rings (involving symmetry factors). If the ring weight is invariant when exchanging the exterior and the interior, then $H(x, y)$ is symmetric in x and y . In all the cases discussed in this paper, $H(x, y)$

thus $A(x, y)$ will be simple rational function of x and y . For instance, in the triangular, quadrangular, rigid and twisting cases discussed above, we have respectively

$$\begin{aligned}
H^{\text{tri}}(x, y) &= \frac{1}{1 - h(x + y)}, & A^{\text{tri}}(x, y) &= \frac{hx}{1 - h(x + y)}, \\
H^{\text{quad}}(x, y) &= \frac{1}{1 - h_1xy - h_2(x^2 + y^2)}, & A^{\text{quad}}(x, y) &= \frac{h_1xy + 2h_2x^2}{1 - h_1xy - h_2(x^2 + y^2)}, \\
H^{\text{rigid}}(x, y) &= \frac{1}{1 - h_1xy}, & A^{\text{rigid}}(x, y) &= \frac{h_1xy}{1 - h_1xy}, \\
H^{\text{twist}}(x, y) &= \frac{1}{1 - h_2(x^2 + y^2)}, & A^{\text{twist}}(x, y) &= \frac{2h_2x^2}{1 - h_2(x^2 + y^2)}.
\end{aligned} \tag{2.10}$$

More generally, if the ring weight is simply given by a product of local face weights (lfw), say $h_{\ell, \ell'}$ per face incident to ℓ external edges and ℓ' internal edges, then $H(x, y)$ corresponds to the generating function for unrooted rings with a distinguished face. Such rings are in correspondence with sequences of faces, so that

$$H^{\text{lfw}}(x, y) = \frac{1}{1 - \sum_{\ell, \ell' \geq 0} h_{\ell, \ell'} x^\ell y^{\ell'}}, \quad A^{\text{lfw}}(x, y) = \frac{\sum_{\ell, \ell' \geq 0} \ell h_{\ell, \ell'} x^\ell y^{\ell'}}{1 - \sum_{\ell, \ell' \geq 0} h_{\ell, \ell'} x^\ell y^{\ell'}}. \tag{2.11}$$

which are rational if the family $(h_{\ell, \ell'})_{\ell, \ell' \geq 0}$ has finite support. The symmetric case corresponds to having $h_{\ell, \ell'} = h_{\ell', \ell}$ for all $\ell, \ell' \geq 0$.

2.3. The functional equation for $O(n)$ loop models

The fixed point condition (2.3), which is an equation for the infinite sequence $(g_k)_{k \geq 1}$, may be rephrased as a functional equation for the *resolvent* of the model, defined as

$$W(x) = \sum_{p \geq 0} \frac{F_p}{x^{p+1}}. \tag{2.12}$$

Recall that F_p is a specialization of the generating function $\mathcal{F}_p(g_1, g_2, \dots)$ for maps with controlled face degrees. As such, the resolvent $W(x)$ satisfies a number of known analytic properties, which we review in Section 6. In particular, when the model is well-defined, that is to say the parameters of the model (n , the $g_k^{(0)}$'s and the w_r 's) are such that the F_p 's are finite, W may be analytically continued into a function that is holomorphic on the complex plane except on a cut where it has a finite discontinuity (see Section 6.1). When all weights are real non-negative, this cut is a real interval $[\gamma_-, \gamma_+]$ with $\gamma_+ \geq |\gamma_-|$. The discontinuity of W on its cut is the so-called *spectral density*

$$\rho(x) = \frac{W(x - i0) - W(x + i0)}{2i\pi} \tag{2.13}$$

which vanishes at $x = \gamma_\pm$. Moreover, as discussed in Section 6.2, we have the fundamental relation

$$W(x + i0) + W(x - i0) = V'(x), \quad x \in]\gamma_-, \gamma_+[, \tag{2.14}$$

where we introduce the shorthand notation

$$V'(x) = x - \sum_{k \geq 1} g_k x^{k-1} . \quad (2.15)$$

This fundamental relation holds for the resolvent of general maps with controlled face degrees, i.e. does not require that the weight sequence $(g_k)_{k \geq 1}$ satisfies the fixed-point condition (2.3). This latter condition (2.3) allows to rewrite $V'(x)$ as

$$\begin{aligned} V'(x) &= x - \sum_{k \geq 1} g_k^{(0)} x^{k-1} - n \sum_{k \geq 1} \sum_{k' \geq 0} A_{k,k'} F_{k'} x^{k-1} \\ &= V'_0(x) - \frac{n}{2i\pi x} \oint_{\mathcal{C}} A(x, y) W(y) dy \end{aligned} \quad (2.16)$$

where $A(x, y)$ is defined as in (2.8), \mathcal{C} is a contour surrounding $[\gamma_-, \gamma_+]$ and

$$V'_0(x) = x - \sum_{k \geq 1} g_k^{(0)} x^{k-1} . \quad (2.17)$$

Note that the contour \mathcal{C} must be included in the domain of analyticity of $y \mapsto A(x, y)$ for all $x \in]\gamma_-, \gamma_+[$. We end up with the linear functional equation

$$W(x + i0) + W(x - i0) = V'_0(x) - \frac{n}{2i\pi x} \oint_{\mathcal{C}} A(x, y) W(y) dy , \quad x \in]\gamma_-, \gamma_+[. \quad (2.18)$$

A new feature of this equation is that W now appears also on the rhs.

2.4. Some examples of functional relations

When $A(x, y)$ is a rational function, we may evaluate the integral in (2.16) using the residue theorem. For instance, in the triangular case, $A^{\text{tri}}(x, y)W(y)$ has by (2.10) one simple pole at $y = h^{-1} - x$, hence we recover the functional equation [5-9]

$$W^{\text{tri}}(x + i0) + W^{\text{tri}}(x - i0) = V'_0(x) - n W^{\text{tri}}(h^{-1} - x). \quad (2.19)$$

Similarly in the rigid case, $A^{\text{rigid}}(x, y)W(y)$ has one simple pole at $y = 1/(h_1 x)$ and a residue 1 at infinity (since $W(y) \sim 1/y$), hence we recover the functional equation [15]

$$W^{\text{rigid}}(x + i0) + W^{\text{rigid}}(x - i0) = V'_0(x) + \frac{n}{x} - \frac{n}{h_1 x^2} W^{\text{rigid}}\left(\frac{1}{h_1 x}\right) . \quad (2.20)$$

In the generic quadrangular case ($h_2 > 0$), $A^{\text{quad}}(x, y)W(y)$ has two simple poles at the roots

$$y_{\pm}(x) = \frac{-h_1 x \pm \sqrt{(h_1^2 - 4h_2^2)x^2 + 4h_2}}{2h_2} \quad (2.21)$$

and the functional equation reads

$$W^{\text{quad}}(x + i0) + W^{\text{quad}}(x - i0) = V'_0(x) + n y'_+(x) W^{\text{quad}}(y_+(x)) + n y'_-(x) W^{\text{quad}}(y_-(x)) . \quad (2.22)$$

Let us now discuss the case where the gasket is a bipartite map, i.e. when all its faces have even degree. Such a situation occurs whenever $g_{2k+1}^{(0)}$ and $A_{2k+1,2k'}$ vanish for all $k, k' \geq 0$, so that $g_{2k+1} = 0$ for all k . Then F_p vanishes for all p odd so that $W(x)$ is an odd function of x (in particular, $\gamma_- = -\gamma_+$). We may then write $W(x) = x \tilde{W}(x^2)$ where $\tilde{W}(X)$ has a cut $[0, \Gamma]$ (with $\Gamma = \gamma_+^2 = \gamma_-^2$) on which it satisfies

$$\tilde{W}(X + i0) + \tilde{W}(X - i0) = \tilde{V}'(X), \quad X \in [0, \Gamma[\quad (2.23)$$

with $\tilde{V}'(X) = 1 - \sum_{k \geq 1} g_{2k} X^{k-1}$. This equation is the bipartite counterpart of (2.14). The fixed point condition (2.3) then yields the functional equation

$$\tilde{W}(X + i0) + \tilde{W}(X - i0) = \tilde{V}'(X) - \frac{n}{2i\pi X} \oint \tilde{A}(X, Y) \tilde{W}(Y) dY \quad (2.24)$$

where the integral is over a contour encircling the cut $[0, \Gamma]$ and

$$\tilde{V}'_0(X) = 1 - \sum_{k \geq 1} g_{2k}^{(0)} X^{k-1}, \quad \tilde{A}(X, Y) = \sum_{k \geq 1} \sum_{k' \geq 0} A_{2k, 2k'} X^k Y^{k'}. \quad (2.25)$$

In particular, in the twisting loop model, $\tilde{A}^{\text{twist}}(X, Y) = A^{\text{twist}}(\sqrt{X}, \sqrt{Y})$ has by (2.10) a simple pole at $Y = h_2^{-1} - X$ with residue 2 so that the functional equation reads

$$\tilde{W}(X + i0) + \tilde{W}(X - i0) = \tilde{V}'_0(X) - 2n \tilde{W}(h_2^{-1} - X), \quad (2.26)$$

which is very similar to (2.19). The solution of the triangular case (2.19) was the topic of the original work of Kostov [5], and Eynard and Kristjansen [8,9]. With identical techniques, the solution for the twisting loop model on quadrangulations (2.26) can be easily deduced (see Section 5). With a few modifications, the method was adapted to solve (2.20) in [15]. In this article, we show how to solve via similar methods a more general family of models (which contains those three examples as special cases).

3. The $O(n)$ loop model on cubic maps with bending energy: equations

3.1. Ring generating functions with one pole

A peculiar feature of the triangular and rigid loop models is that both the ring generating functions $A^{\text{tri}}(x, y)$ and $A^{\text{rigid}}(x, y)$, as defined in (2.10), are rational functions with one pole, which leads to a simplification of the functional equation (2.18) into respectively (2.19) and (2.20). In this section, we put those two models under

the same roof by considering the general “one-pole case” (note that the bipartite ring generating function $\tilde{A}^{\text{twist}}(X, Y)$ is also a one-pole rational function but, for simplicity, we postpone the discussion of the twisting loop model to Section 5).

More precisely, let us first assume that the ring weight is symmetric and does not depend on the position of the distinguished edge, so that $A(x, y)$ is given by (2.9), with $H(x, y)$ a symmetric function. Let us moreover assume that $H(x, y)$ be a one-pole rational function of the form

$$H(x, y) = \frac{h(y)}{x - s(y)}, \quad (3.1)$$

so that $A(x, y)$ is also a one-pole rational function in x . Note that to fulfill this latter condition, it is important that the numerator does not depend on x , since any zero of the numerator would give rise to an extra pole in $A(x, y)$. Demanding that $H(x, y)$ be symmetric in x, y yields a functional equation for h and s . It is readily solved (e.g. write the equation for $y = 0$ and solve for $h(x)$, then substitute into the equation for $y = 1$) and implies that $s(x)$ takes the form

$$s(x) = \frac{\alpha - \beta x}{\beta - \delta x} \quad (3.2)$$

for some real parameters α, β and δ , while $h(x) \propto 1/(\alpha - \beta x)$. Note the remarkable property $s(s(x)) = x$. In other words, we recognize in (3.2) the general expression for a *homographic involution*. In particular, this involution reduces to $s(x) = h^{-1} - x$ for the triangular model and to $s(x) = 1/(h_1 x)$ for the rigid model. By (2.9), we have

$$A(x, y) = \frac{x}{s(y) - x} \quad (3.3)$$

hence the ring generating function $A_{k, k'}$ satisfies the *exponentiation property*

$$\sum_{k' \geq 0} A_{k, k'} y^{k'} = s(y)^{-k}, \quad k \geq 1. \quad (3.4)$$

For positive ring weights, $s(y)$ is then necessarily a decreasing positive function of the real positive variable y . This imposes $s(0) > 0$ together with the extra condition $\beta^2 - \alpha\delta > 0$. Hence, the involution has two real fixed points at $(\beta \pm \sqrt{\beta^2 - \alpha\delta})/\delta$. We will see in the next subsection that all the decreasing homographic involutions are indeed obtained in a simple model of loops with bending energy. In Appendix A, we mention the cases where the homographic involution is increasing, although they cannot be reached with non-negative local weights.

By the form (3.2) for $s(x)$, one may easily check that $A(x, y)$, as given by (3.3), may be written in the alternative form

$$A(x, y) = \frac{xs'(x)}{y - s(x)} + \frac{xs''(x)}{2s'(x)}, \quad (3.5)$$

which displays its single pole in the variable y at $y = s^{-1}(x) = s(x)$. We may now evaluate the contour integral in (2.18) via the residue theorem. Recall that, in order for the model to be well-defined, the cut $[\gamma_-, \gamma_+]$ of W has to be contained, for all x on the cut, within the disk of convergence of $y \mapsto A(x, y)$ which here has radius $|s(x)|$. This shows that the interior of the cut may not overlap with its image under s (but the endpoints of the cut may be fixed points of s). The integrand $A(x, y)W(y)$ has a pole at $y = s(x)$, with residue equal to $-xs'(x)W(s(x))$. Since $W(y) \sim 1/y$ for $y \rightarrow \infty$, the residue at infinity is equal to $\lim_{y \rightarrow \infty} A(x, y) = xs''(x)/(2s'(x))$. We deduce that

$$\frac{1}{2i\pi} \oint A(x, y)W(y)dy = -xs'(x)W(s(x)) + \frac{xs''(x)}{2s'(x)} \quad (3.6)$$

which, inserted in (2.18), yields the functional equation

$$W(x + i0) + W(x - i0) - ns'(x)W(s(x)) = V_0'(x) - \frac{ns''(x)}{2s'(x)}, \quad x \in]\gamma_-, \gamma_+[\quad (3.7)$$

This equation generalizes eqs. (2.19) and (2.20), which are recovered respectively for $s(x) = h^{-1} - x$ and $s(x) = 1/(h_1x)$, as expected.

3.2. Realization in a model of loops with bending energy

In this Section, we exhibit a model whose ring generating function reproduces precisely the most general symmetric one-pole rational function of the previous subsection, hence whose resolvent is the solution of the general functional equation (3.7). We consider again an $O(n)$ loop model where the loops visit only triangles, with a weight h per visited triangle, but we also introduce a *bending energy* for the loops in the following way: each triangle visited by a loop has exactly one edge which is not crossed by the loop. We say that the triangle faces outwards (resp. inwards) if this edge is on the same side of the loop as the external face (resp. on the opposite side). Now for each *pair* of successive triangles along a loop, we attach a weight a if the triangles are of the same nature (either both facing outwards or both facing inwards) and a weight 1 otherwise. We may interpret $-\log a$ as a bending energy for the loops as this new weight favors loop turns for $a > 1$ and penalizes them for $0 < a < 1$. Such a bending energy was previously introduced in [17] in the different context of Lorentzian triangulations. Note that our model precisely interpolates between the regular $O(n)$ loop model on triangles, recovered for $a = 1$, and the rigid $O(n)$ loop model on squares, recovered for $a = 0$ and $h_1 = h^2$. Indeed, at $a = 0$, outward- and inward-facing triangles necessarily alternate along the loop and, upon concatenating them by pairs, we may simply replace them by squares (with weight h^2) having opposite sides crossed by the loop.

Let us now compute the ring grand generating function $A(x, y)$. Rings whose inner contour has zero length are non-empty sequences of outward-facing triangle only, each triangle receiving a weight ahx . These rings therefore have a grand generating function equal to $\frac{ahx}{1-ahx}$. Rings with inner contour of non-zero length may be viewed, before choosing their root edge, as cyclic sequences of composite objects consisting of (i) a

non-empty sequence of outward-facing triangles followed by (ii) a non-empty sequence of inward-facing triangles. Each composite object therefore yields a grand generating function $\frac{hx}{1-ahx} \cdot \frac{hy}{1-ahy}$ (with no weight a for the first triangle of each sequence since it follows a triangle of the opposite type). We deduce eventually

$$A(x, y) = \frac{ahx}{1-ahx} + x \frac{\partial}{\partial x} \left(-\log \left(1 - \frac{hx}{1-ahx} \frac{hy}{1-ahy} \right) \right) \quad (3.8)$$

where, in the second term, the $\log(\cdot)$ accounts for the cyclic sequence of composite objects while the $x\partial_x$ accounts for the rooting of the ring. We observe that $A(x, y)$ is indeed of the form (2.9) with

$$H(x, y) = \frac{1}{1-ah(x+y) - (1-a^2)h^2xy} \quad (3.9)$$

which is a symmetric one-pole rational function (observe the similarity with Eq. (2.3) of [17]). We are therefore precisely in the situation discussed in Section 3.1, hence we may rewrite $A(x, y)$ in the forms (3.3) and (3.5) with $s(x)$ now given by

$$s(x) = \frac{1-ahx}{ah + (1-a^2)h^2x} \quad (3.10)$$

which has two fixed points at $x = \frac{1}{(a\pm 1)h}$. We therefore recover the general form (3.2) for an arbitrary decreasing homographic involution such that $s(0) > 0$ (with $\frac{1}{s(0)} = \frac{\beta}{\alpha} = ha$, $\frac{\delta}{\alpha} = (a^2 - 1)h^2$, $\beta^2 - \alpha\delta = h^2\alpha^2 > 0$). In other words, our loop model with bending energy realizes precisely the general “one-pole” case. Note that $s(x)$ reduces to $h^{-1} - x$ for $a = 1$ and to $\frac{1}{h^2x}$ for $a = 0$, as it should.

3.3. Solving strategy

The technique developed by Eynard and Kristjansen [8] to solve the functional equation (2.19) may be adapted to (3.7) with few modifications, as we will now sketch. Briefly, we may see that, for fixed given γ_{\pm} , the functional equation admits a unique solution W analytic outside the cut $[\gamma_-, \gamma_+]$ and such that $W(x) \sim 1/x$ for $x \rightarrow \infty$. Then, the unknowns γ_{\pm} are determined *a posteriori* by the condition $\rho(\gamma_{\pm}) = 0$, where ρ is the spectral density (2.13).

We will restrict ourselves to the case where V'_0 is a polynomial, i.e. we assume that the degrees of the faces not visited by loops are also bounded. In that case, V'_0 is defined on the whole complex plane, and we easily find a particular solution of (3.7) with no discontinuity along the cut, namely

$$W_{\text{part}}(x) = \frac{2V'_0(x) + ns'(x)V'_0(s(x))}{4-n^2} - \frac{ns''(x)}{2(n+2)s'(x)}. \quad (3.11)$$

To check that this is indeed a particular solution, note that, $s(x)$ being an involution, we have $s'(s(x)) = 1/s'(x)$ and $s''(s(x)) = -s''(x)/s'(x)^3$. Since V'_0 is a polynomial,

observe that W_{part} has (multiple) poles at ∞ and at $s(\infty)$. Any solution of (3.7) is of the form

$$W(x) = W_{\text{part}}(x) + W_{\text{hom}}(x) , \quad (3.12)$$

where W_{hom} is now a solution of the homogeneous functional equation

$$W_{\text{hom}}(x + i0) + W_{\text{hom}}(x - i0) - n s'(x) W_{\text{hom}}(s(x)) = 0 , \quad x \in]\gamma_-, \gamma_+[. \quad (3.13)$$

Assuming that $s(\infty) \neq \infty$, viz. $\delta \neq 0$ in (3.2) and $a \neq 1$ in (3.10), the requirement $W(x) \sim 1/x$ for $x \rightarrow \infty$ yields the condition

$$W_{\text{hom}}(x) = -W_{\text{part}}(x) + \frac{1}{x} + O\left(\frac{1}{x^2}\right) = -\frac{2V_0'(x)}{4-n^2} + \frac{2}{n+2} \frac{1}{x} + O\left(\frac{1}{x^2}\right) . \quad (3.14)$$

Moreover, the analyticity of W outside the cut, and the fact that W is bounded in some neighborhood of the cut, require that the pole of W_{part} at $s(\infty)$ is canceled, which may be rephrased as

$$\begin{aligned} s'(x)W_{\text{hom}}(s(x)) &= -s'(x)W_{\text{part}}(s(x)) + O\left(\frac{1}{x^2}\right) = -\frac{nV_0'(x)}{4-n^2} + \frac{n}{n+2} \frac{1}{x} + O\left(\frac{1}{x^2}\right) \\ &= \frac{n}{2}W_{\text{hom}}(x) + O\left(\frac{1}{x^2}\right) \end{aligned} \quad (3.15)$$

when $x \rightarrow \infty$. When $s(\infty) = \infty$, viz. $\delta = 0$ in (3.2) or $a = 1$ in (3.10), the two conditions (3.14) and (3.15) are replaced by the single condition

$$W_{\text{hom}}(x) = -W_{\text{part}}(x) + \frac{1}{x} + O\left(\frac{1}{x^2}\right) = -\frac{2V_0'(x) + ns'(x)V_0'(s(x))}{4-n^2} + \frac{1}{x} + O\left(\frac{1}{x^2}\right) . \quad (3.16)$$

The general solution of (3.13) may be expressed in terms of elliptic functions: let us introduce the elliptic integral

$$v(x) = \int_x^{s(\gamma_-)} \frac{d\xi}{\sqrt{\pm(\xi - \gamma_+)(\xi - \gamma_-)(\xi - s(\gamma_+))(\xi - s(\gamma_-))}} . \quad (3.17)$$

Since s is (locally) decreasing and the cut $[\gamma_-, \gamma_+]$ does not overlap with its image, the sign may be chosen in such a way that the polynomial under the square root be positive over $[s(\gamma_+), s(\gamma_-)]$ (when $s(\gamma_+) > s(\gamma_-)$, this interval is to be understood as the union $] - \infty, s(\gamma_-)] \cup [s(\gamma_+), \infty[$). In particular, this implies that $T = v(s(\gamma_+))$ is real and positive. By the same reason, the polynomial under the square root is negative on $[s(\gamma_-), \gamma_-]$ (understood as $] - \infty, \gamma_-] \cup [s(\gamma_-), \infty[$ if $\gamma_- < s(\gamma_-)$) so that $v(\gamma_-)$ has two pure imaginary determinations $\pm iT'$ ($T' > 0$). Finally, we may check that $v(\gamma_+) = T \pm iT'$.

For the moment, we assume that $s(\gamma_{\pm}) \neq \gamma_{\pm}$ so that $T < \infty$. The function $x \mapsto v(x)$ has branch points of order 2 at $\gamma_{\pm}, s(\gamma_{\pm})$ and maps the lower (resp. upper)

half-plane onto the rectangle $[0, T] + i[0, T']$ (resp. $[0, T] + i[-T', 0]$). Its reciprocal function $v \mapsto x(v)$ may be analytically continued to an even, doubly periodic function with periods $2T$ and $2iT'$, with simple poles at $\pm v_\infty \bmod 2T\mathbf{Z} + 2iT'\mathbf{Z}$, where $v_\infty = \lim_{x \rightarrow \infty} v(x)$. Note the fundamental property

$$x(v \pm iT') = s(x(v)) \quad (3.18)$$

which follows from (3.17): indeed, considering $v(s(x))$, the change of variable $\xi \rightarrow s(\xi)$ leaves the integrand invariant (here it is crucial that s be a homographic involution) and sets the endpoints of the integration path to x and γ_- respectively, so that $v(s(x)) = v(x) - v(\gamma_-)$.

For v in the strip $] -\infty, \infty[+ i] - T', T'[$ (which is mapped onto the complement of the cut $[\gamma_-, \gamma_+]$), let us define

$$\omega(v) = x'(v) W_{\text{hom}}(x(v)) . \quad (3.19)$$

Since W_{hom} is meromorphic outside the cut $[\gamma_-, \gamma_+]$, ω is meromorphic on the strip. Note that ω is odd and $2T$ -periodic. Furthermore, by the above mapping property of x , we find that ω has well-defined values on the boundary of the strip, namely

$$\omega(v \pm iT') = x'(v \pm iT') W_{\text{hom}}(x(v \pm iT') \mp i0), \quad 0 < v < T \quad (3.20)$$

(the value of $\omega(v \pm iT')$ for other real values of v follows by oddness and $2T$ -periodicity). By (3.13) and (3.18) (and its derivative), we deduce that, for any real v ,

$$\omega(v + iT') + \omega(v - iT') - n\omega(v) = 0 . \quad (3.21)$$

This relation implies that ω may be analytically continued into a meromorphic function defined on the whole complex plane, so that (3.21) holds for all complex values of v . For simplicity, we assume now $n \neq \pm 2$ (for $n = -2, 2$, the solution is also known, see for instance [6] but we will not discuss it here). As discussed in [15], any $2T$ -periodic meromorphic solution of (3.21) can be expressed in terms of the ‘‘fundamental’’ solutions $\zeta_{\pm b}$, where $\pi b = \arccos(n/2)$ and

$$\zeta_b(v) = \frac{\vartheta_1'(0|\tau)}{2T \vartheta_1(-\frac{b}{2}|\tau)} \frac{\vartheta_1(\frac{v}{2T} - \frac{b}{2}|\tau)}{\vartheta_1(\frac{v}{2T}|\tau)}, \quad \tau = \frac{iT'}{T} \quad (3.22)$$

(see the Appendix in [15] for some properties of $\zeta_b(v)$). More precisely, any $2T$ -periodic solution of (3.21) is a linear combination of derivatives of translates of $\zeta_{\pm b}$. Here, we are looking for an odd solution with poles at $\pm v_\infty$ whose residues are fixed, when $s(\infty) \neq \infty$, by the condition

$$\omega(v) = x'(v) \left(-\frac{2V_0'(x(v))}{4 - n^2} + \frac{2}{n + 2} \frac{1}{x(v)} \right) + o\left(\frac{1}{v - v_\infty} \right) \quad \text{for } v \rightarrow v_\infty \quad (3.23)$$

inherited from (3.14), as well as poles at $\pm v_\infty \pm iT'$ with *the same residues multiplied by $n/2 = \cos \pi b$* by virtue of (3.15). The general form for such a solution is

$$\omega(v) = \sum_{k \geq 0} a_k \left(\zeta^{(k)}(v - v_\infty) - \zeta^{(k)}(-v - v_\infty) \right) \quad (3.24)$$

where

$$\zeta(v) = \frac{\zeta_b(v) + \zeta_{-b}(v)}{2}, \quad (3.25)$$

and where the coefficients a_k are determined by (3.23). Note that the particular combination ζ was chosen as it has residue 1 at 0 and residue $n/2$ at $\pm iT'$ so that (3.23) implies both (3.14) and (3.15). In the case $s(\infty) = \infty$ (hence $v_\infty = iT'/2$), the condition (3.23) has to be modified according to (3.16). We may observe that only a finite number of a_k 's are non-zero when V'_0 is a polynomial. More precisely, when the maximal allowed face degree is D , then $a_k = 0$ for $k > D$.

After determining ω in this way, it remains to satisfy the conditions $\rho(\gamma_\pm) = 0$. By (3.20), we may rewrite the spectral density (2.13) in the parametric form

$$\rho(x(v + iT')) = \frac{\omega(v + iT') - \omega(v - iT')}{2i\pi x'(v + iT')}, \quad 0 < v < T. \quad (3.26)$$

Since x has ramifications points of order 2 at iT' and $T + iT'$, the conditions $\rho(\gamma_\pm) = 0$ amount to $\omega(iT') = \omega(T + iT') = 0$, which implicitly determine γ_\pm .

We further deduce that ρ (hence W) has generically a square-root singularity at γ_\pm , corresponding to a non-critical point in the terminology reviewed in Section 6.1. For $T < \infty$, a critical point may only be obtained when ω'' vanishes at either iT' or $T + iT'$, so that ρ now decays generically with an exponent $3/2$ at one endpoint of the cut: this corresponds to a generic critical point, in the universality class of pure gravity. Multicritical points can also be obtained, but only at the price of introducing negative weights in the model.

The only possible way to obtain a non-generic critical point with non-negative weights is to have $\gamma_+ = s(\gamma_+)$, so that $T = \infty$. The above strategy simplifies greatly in this situation. Indeed, since one of the periods ($2T$) is infinite, the elliptic (doubly periodic) parametrization degenerates into a (simply periodic) trigonometric parametrization (see Fig. 2). It is then convenient to rescale v by a constant factor so that $v(\gamma_-) = \pm i\pi$ (i.e. $T' = \pi$). The reciprocal function $v \mapsto x(v)$ then reads explicitly

$$x(v) = (\gamma_+ - s(\gamma_-)) \frac{\cosh v - 1}{\cosh v - \cosh v_\infty} + s(\gamma_-) \quad (3.27)$$

where v_∞ is determined by the condition $x(i\pi) = \gamma_-$. Furthermore, for $T = \infty$ and $0 < n < 2$, the fundamental solution ζ in (3.25) reads

$$\zeta(v) = \cosh(bv) \coth v - \sinh(bv) \quad (3.28)$$

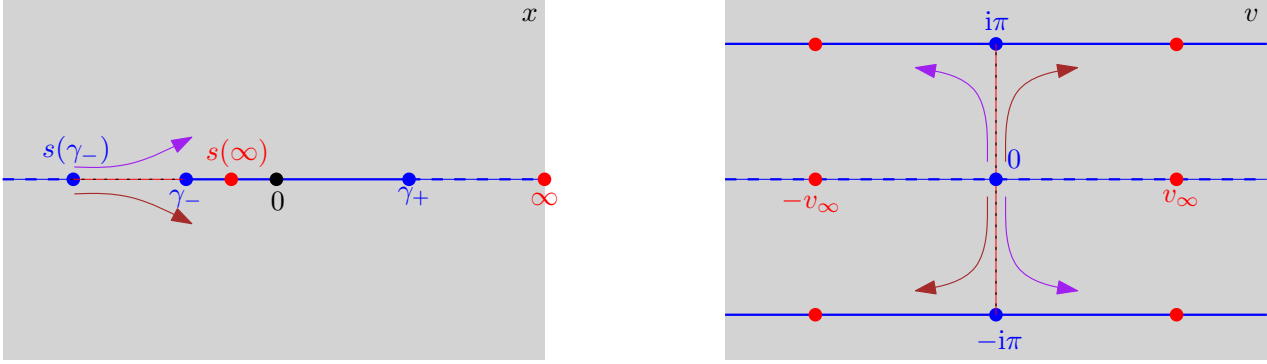


Fig. 2: The (multivalued) change of variable from x to v , as given by (3.17) in the particular case $\gamma_+ = s(\gamma_+)$, up some normalization factor which ensures that $v(\gamma_-) = \pm i\pi$. The reciprocal function is given by Eq. (3.27). Here we assumed that $s(\infty)$ belongs to the cut $]\gamma_-, \gamma_+[$ (solid line) so that the image (in the x -plane) of this cut by the involution s is $]-\infty, s(\gamma_-)[\cup]\gamma_+, \infty[$ (dashed line). The cut maps onto the lines $\text{Im } v = \pm\pi$ in the v -plane (solid lines), while its image maps onto the line $\text{Im } v = 0$ (dashed line).

with

$$\pi b = \arccos\left(\frac{n}{2}\right). \quad (3.29)$$

Hence we may apply the above strategy on very explicit formulas. The only caution we must take concerns the condition $\rho(\gamma_+) = 0$ which, since $x'(v) \sim Ce^{-v}$ for $v \rightarrow \infty$, now amounts to the condition $\omega(v) = o(e^{-v})$. Noting that ζ has the asymptotic expansion

$$\zeta(v) = e^{-bv} + e^{-(2-b)v} + e^{-(2+b)v} + o(e^{-(2+b)v}) \quad (3.30)$$

with $0 < b < 1/2$, this yields a linear condition on the a_k 's appearing in (3.24), that replaces the previous condition $\omega(T + iT') = 0$.

Interestingly, this asymptotic expansion also yields the non-generic critical exponents. Indeed, we generically have $\omega(v) \sim C'e^{-(2-b)v}$ for $v \rightarrow \infty$ and, noting that $x(v) = \gamma_+ + \alpha e^{-v} + o(e^{-v})$ with $\alpha > 0$ (since $x(v)$ approaches γ_+ from the right when v takes large real values), we deduce that $W_{\text{hom}}(x) \sim -\alpha^{b-2}C'(x - \gamma_+)^{1-b}$. This is nothing but the leading singular term in the expansion of W around γ_+ , and the exponent $1 - b$ is characteristic of the universality class of the *dense $O(n)$ loop model on random maps*. By transfer theorems, it amounts to the asymptotic behaviour

$$F_k \sim -\frac{\gamma_+^{1-b}C'}{\alpha^{2-b}\Gamma(b-1)} \frac{\gamma_+^k}{k^{2-b}}, \quad k \rightarrow \infty. \quad (3.31)$$

Since $0 < b < 1/2$, the positivity of F_k (in a model with non-negative weights) requires that $C' \geq 0$. When $C' = 0$, we instead have $\omega(v) \sim C''e^{-(2+b)v}$ so that $W_{\text{hom}}(x) \sim$

$-\alpha^{-b-2}C''(x-\gamma_+)^{1+b}$, and the exponent $1+b$ is characteristic of the universality class of the *dilute $O(n)$ loop model on random maps*. It corresponds to the asymptotic behaviour

$$F_k \sim -\frac{\gamma_+^{1+b}C''}{\alpha^{2+b}\Gamma(-(b+1))} \frac{\gamma_+^k}{k^{2+b}}, \quad k \rightarrow \infty \quad (3.32)$$

hence $C'' < 0$ in a model with non-negative weights. It is not possible to have both $C' = 0$ and $C'' = 0$ in a such a model, thus (3.31) and (3.32) are the only possible “physical” non-generic critical behaviours.

4. The $O(n)$ loop model on cubic maps with bending energy: phase diagram

4.1. The non-generic critical line

In this section, we compute the non-generic critical line of the $O(n)$ loop model with bending energy defined in Section 3.2. As discussed in Section 3.3, non-generic criticality amounts to the condition $s(\gamma_+) = \gamma_+$. Note that γ_+ is a continuous increasing function of the weights $g_k^{(0)}$ and h , with $\gamma_+ = 0$ when the weights vanish. Then, when h is positive and a non-negative, this condition occurs when γ_+ reaches the smallest (in modulus) fixed point of the involution, namely

$$\gamma_+ = \frac{1}{(a+1)h}. \quad (4.1)$$

Note that the other (largest in modulus) fixed point $\frac{1}{(a-1)h}$ of the involution does not necessarily coincide with the other endpoint γ_- of the cut, but lies outside of both the cut and its image. The arguments of Section 6 shows that $\gamma_- = \frac{1}{(a-1)h}$ can happen iff $a = 0$ and the maps are bipartite.

We now apply the strategy of Section 3.3 in the non-generic critical case. The trigonometric parametrization (3.27) reads here, for $a \neq 1$,

$$x(v) = \frac{1}{(1-a^2)h} \frac{(1-a)\cosh v + (1+a)\cosh v_\infty}{\cosh v - \cosh v_\infty}, \quad (4.2)$$

where

$$v_\infty = \arg \cosh \frac{(1-a)(1-(1+a)h\gamma_-)}{(1+a)(1+(1-a)h\gamma_-)}. \quad (4.3)$$

The case $a = 1$ is obtained by taking a suitable limit, which we will discuss in the next section. Note that, since $\cosh v_\infty$ is real, v_∞ necessarily lies on the boundary of the domain $[0, \infty[+ i[0, \pi]$.

Using this explicit parametrization, we may now determine the resolvent exactly, by computing the coefficients in (3.24). From now on, we will focus on the case where

$g_k^{(0)} = g\delta_{k,3}$, i.e. where faces not visited by the loops are themselves triangles, weighted by g . We have in this case $V_0'(x) = x - gx^2$ so that (3.23) can be expanded into

$$\omega(v) = \frac{1}{(4-n^2)(1-a^2)^3} \left\{ -6 \frac{A_3 \frac{g}{h^3}}{(v-v_\infty)^4} + 2 \frac{A_2 \frac{g}{h^3} + B_2 \frac{1}{h^2}}{(v-v_\infty)^3} - \frac{A_1 \frac{g}{h^3} + B_1 \frac{1}{h^2}}{(v-v_\infty)^2} + \frac{C_0}{(v-v_\infty)} + O(1) \right\} \quad (4.4)$$

with

$$\begin{aligned} A_3 &= \frac{8 \coth^3 v_\infty}{3} \\ A_2 &= 8 \coth^2 v_\infty (a + \sinh^{-2} v_\infty) \\ B_2 &= 4 \coth^2 v_\infty (1 - a^2) \\ A_1 &= \frac{4 \coth v_\infty}{3} (6 \coth^4 v_\infty + (6a - 8) \coth^2 v_\infty + 3(1 - a^2)) \\ B_1 &= 4 \coth v_\infty (1 - a^2) (\coth^2 v_\infty - (1 - a)) \\ C_0 &= 2(1 - a^2)^3 (n - 2). \end{aligned} \quad (4.5)$$

Then, since the fundamental solution ζ in (3.28) has a simple pole at 0 with residue 1, satisfying (4.4) leads us immediately to the desired expression for ω :

$$\begin{aligned} \omega(v) &= \frac{1}{(4-n^2)(1-a^2)^3} \left\{ A_3 \frac{g}{h^3} (\zeta'''(v-v_\infty) - \zeta'''(-v-v_\infty)) \right. \\ &\quad + \left(A_2 \frac{g}{h^3} + B_2 \frac{1}{h^2} \right) (\zeta''(v-v_\infty) - \zeta''(-v-v_\infty)) \\ &\quad + \left(A_1 \frac{g}{h^3} + B_1 \frac{1}{h^2} \right) (\zeta'(v-v_\infty) - \zeta'(-v-v_\infty)) \\ &\quad \left. + C_0 (\zeta(v-v_\infty) - \zeta(-v-v_\infty)) \right\}. \end{aligned} \quad (4.6)$$

In order for the solution (4.6) to be consistent, we should ensure that the spectral density ρ vanishes at γ_\pm . As discussed in Section 3.3, demanding that $\rho(\gamma_-) = 0$ amounts to the condition

$$\omega(i\pi) = 0 \quad (4.7)$$

where, from (4.6),

$$\begin{aligned}
\omega(i\pi) \propto & A_3 \frac{g}{h^3} \left(b \cosh(bv_\infty) \coth v_\infty \left(b^2 + 6 \sinh^{-2} v_\infty \right) \right. \\
& \left. - (2 \sinh^{-4} v_\infty + (3b^2 + 4 \coth^2 v_\infty) \sinh^{-2} v_\infty + b^3) \sinh(bv_\infty) \right) \\
& + \left(A_2 \frac{g}{h^3} + B_2 \frac{1}{h^2} \right) (b \cosh(bv_\infty) (2 \sinh^{-2} v_\infty + b) - \coth v_\infty (b^2 + 2 \sinh^{-2} v_\infty) \sinh(bv_\infty)) \\
& + \left(A_1 \frac{g}{h^3} + B_1 \frac{1}{h^2} \right) \left(\frac{1}{2} \sinh^{-2} v_\infty ((b-2) \sinh(bv_\infty) - b \sinh((b-2)v_\infty)) \right) \\
& + C_0 \sinh^{-1} v_\infty \sinh((1-b)v_\infty) .
\end{aligned} \tag{4.8}$$

Similarly, demanding that $\rho(\gamma_+) = 0$ amounts, as already discussed, to the condition

$$\omega(v) = o(e^{-v}) \quad \text{for } v \rightarrow +\infty. \tag{4.9}$$

By (3.30) and (4.6), we have the asymptotic expansion

$$\omega(v) = \kappa(b)e^{-bv} + \kappa(2-b)e^{-(2-b)v} + o(e^{-(2-b)v}) \tag{4.10}$$

with

$$\begin{aligned}
\kappa(b) = & \frac{1}{(4-n^2)(1-a^2)^3} \left\{ A_3 \frac{g}{h^3} (-2b^3 \sinh(bv_\infty)) + \left(A_2 \frac{g}{h^3} + B_2 \frac{1}{h^2} \right) (2b^2 \cosh(bv_\infty)) \right. \\
& \left. + \left(A_1 \frac{g}{h^3} + B_1 \frac{1}{h^2} \right) (-2b \sinh(bv_\infty)) + C_0 (2 \cosh(bv_\infty)) \right\} .
\end{aligned} \tag{4.11}$$

Then, the condition (4.9) reads nothing but

$$\kappa(b) = 0 . \tag{4.12}$$

Finally, the positivity of the F_k 's requires by (3.31) the extra condition

$$\kappa(2-b) \geq 0. \tag{4.13}$$

4.2. Phase diagram

Fixing $a \geq 0$ and b strictly between 0 and 1/2 (i.e. $0 < n < 2$), the consistency conditions (4.7), (4.12) and (4.13) determine the values of g and h where the model is non-generic critical. Viewing v_∞ as a parameter, (4.7) and (4.12) form a system of inhomogeneous linear equations for the variables g/h^3 and $1/h^2$ (or equivalently for the variables g/h and h^2 after multiplying the equations by h^2). Solving this system, we obtain a family of non-generic critical points, forming a line in the (g, h) plane parametrized by v_∞ . Recall that $\cosh v_\infty$ is real, so that v_∞ varies on $[0, \infty] \cup [i[0, \pi]) \cup$

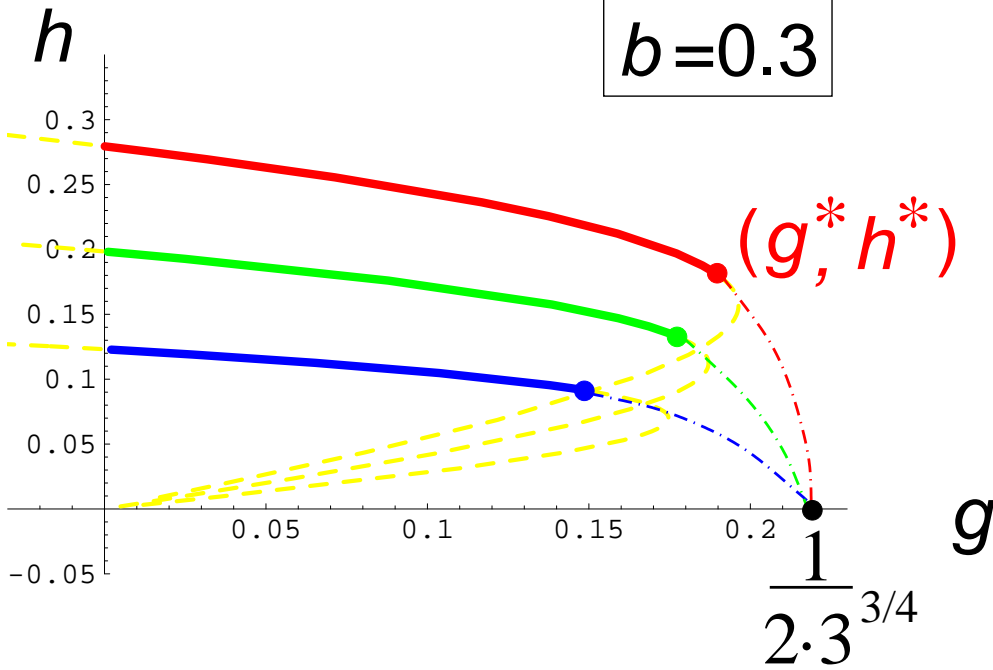


Fig. 3: Phase diagram of the $O(n)$ loop model with bending energy in the (g, h) plane. The various plots correspond to $b = 0.3$ ($n = 2 \cos \pi b$) and, from top to bottom, $a = 0.5$ (red), 1 (green) and 2 (blue). Plots for other values of b and $a < a_c(n)$ would essentially have the same aspect. The solid line corresponds to non-generic critical models and is *computed exactly* upon solving eqs.(4.7) and (4.12). In the absence of the third constraint (4.13), this line would continue as indicated in dashed line (yellow). The condition (4.13) imposes that the line terminates at a point (g^*, h^*) . All points on the non-generic critical line lie in the universality class of the dense $O(n)$ model except the endpoint (g^*, h^*) which lies in the universality class of a dilute $O(n)$ model. For the various models, a dot-dashed line was drawn (but not computed exactly here) to represent the line of generic critical points. This line connects the point (g^*, h^*) to the point $(\frac{1}{2.3^{3/4}}, 0)$ describing pure triangulations. The model is well-defined for values of g and h lying below the (generic or non-generic) critical lines. The non-generic critical line reduces to a single dilute point with $g^* = 0$ at $a = a_c(n)$, and vanishes for $a > a_c(n)$.

$([0, \infty[+i\pi)$. This range is further restricted by the requirement that $g \geq 0$ and $h \geq 0$, and by the condition (4.13). We do not give here the precise parametrization of the non-generic critical line as the formulas are quite cumbersome, but we instead present in Fig. 3 the corresponding plots for $b = 0.3$ and several values of a . Plots for other values of b and a (not too large) have essentially the same aspect: the line starts at $g = 0$ and a finite value of h and ends at a point (g^*, h^*) . The value of g^* decreases with increasing a and reaches 0 for a threshold value $a = a_c(n)$. For $a > a_c(n)$, the non-generic critical line disappears. The value of $a_c(n)$ decreases with increasing n from

0 to 2, with the particular values $a_c(0) = \infty$, $a_c(1) = 4$ and $a_c(2) = 2$. The physical meaning of this phenomenon is under investigation.

For $a < a_c(n)$, all points on the non-generic critical line, except the endpoint (g^*, h^*) , lie in the universality class of the dense $O(n)$ model: in particular F_k has the asymptotic behaviour (3.31) (with $C' = \kappa(2-b) > 0$). The endpoint (g^*, h^*) lies instead in the universality class of the dilute $O(n)$ model: F_k has the asymptotic behaviour (3.32) (with $C'' = \kappa(2+b) < 0$). On the plots, we have also indicated the existence of a line of generic critical points which links the point (g^*, h^*) to the generic critical point of pure triangulations without loops, obtained for $h = 0$ and $g = 1/(2 \cdot 3^{3/4})$. An explicit parametric representation for this line can be also obtained by the strategy of Section 2.5, but its expression is even more cumbersome than that of the non-generic critical line (see for instance [15, Section 6.4] for its computation in the $a = 0$ case, with different face weights of the form $g_k^{(0)} = g\delta_{k,4}$).

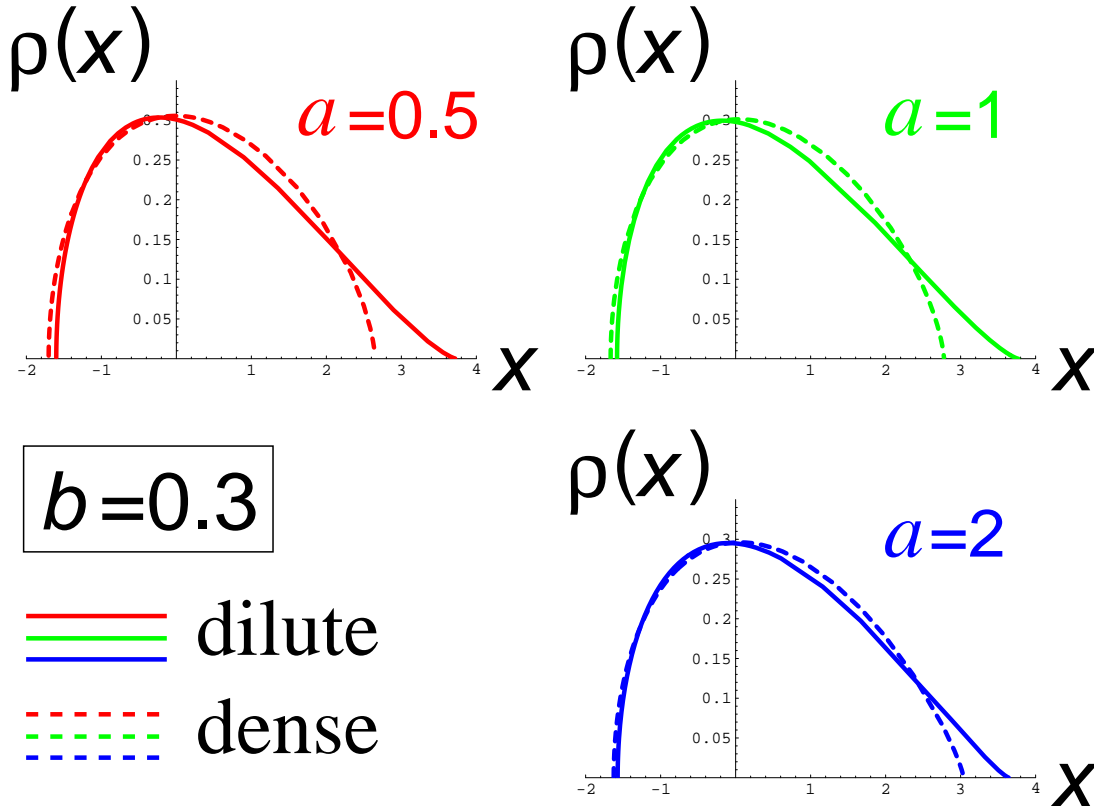


Fig. 4: Plots of the spectral density of the $O(n)$ loop model with bending energy at $b = 0.3$ and for $a = 0.5, 1$ and 2 . For each case, we plotted the spectral density at the non-generic critical dilute point (g^*, h^*) (solid line), and at some (somewhat arbitrary) non-generic critical dense point along the non-generic critical line (dashed line).

For illustration, we have plotted in Fig. 4 the spectral density of eq. (3.26) at the dilute point and at some (arbitrarily chosen) dense point on the non-generic critical line

for $b = 0.3$ and for the three values of a displayed in Fig. 3.

As already mentioned, the case $a = 1$ is special. Still, the equation of the non-generic critical line may in practice be obtained by simply taking the $a \rightarrow 1$ limit of the consistency conditions (4.7), (4.12) and (4.13), with v_∞ tending simultaneously to $i\pi/2$ as

$$v_\infty = \frac{i\pi}{2} + i(a-1) \left(\frac{1}{2} - h\gamma_- \right) + O((a-1)^2) \quad (4.14)$$

so that Eq. (4.3) remains satisfied. Solving the first two conditions in this limit leads to the following parametrization of the non-generic critical line

$$\begin{aligned} \frac{g}{h} &= \frac{2b\sqrt{2+n}\rho - 2\sqrt{2-n}}{2b\sqrt{2+n}\rho - \sqrt{2-n}(1 + \frac{1-b^2}{2}\rho^2)} \\ h^2 &= \frac{b\rho^2}{48\sqrt{4-n^2}} \frac{b\sqrt{2+n}(6 + (1-b^2)\rho^2) - 4(1-b^2)\sqrt{2-n}\rho}{2b\sqrt{2+n}\rho - \sqrt{2-n}(1 + \frac{1-b^2}{2}\rho^2)}, \end{aligned} \quad (4.15)$$

where we use $\rho = 1 - 2h\gamma_- = 1 - \frac{\gamma_-}{\gamma_+} \geq 0$ as a parameter along the line. The corresponding plot is displayed in Fig. 3. From the third condition, we find that the line ends at the dilute point

$$\frac{g^*}{h^*} = 1 + \sqrt{\frac{2-n}{6+n}}, \quad (h^*)^2 = \frac{(2-b)b}{12(1-b)^2} \frac{4 - \sqrt{(2-n)(6+n)}}{(2+n)\sqrt{(2-n)(6+n)}}. \quad (4.16)$$

These formulas are in agreement with the results of [5]. In particular, we find the value $h = \frac{1}{2\sqrt{2}\sqrt{2+n}}$ for the non-generic critical point at $g = 0$, with $\gamma_- = \sqrt{2}\sqrt{2+n}(1 - \frac{\sqrt{2-n}}{b})$ at this point.

For $n = 1$ ($b = 1/3$) and $a = 1$, the model is equivalent to the Ising model on the vertices of a random triangulation at zero magnetic field, as seen by viewing the loops as domain walls for the Ising spins. Besides the point $g^* = \frac{\sqrt{5}}{2\sqrt{2}\cdot 7^{3/4}}$, $h^* = \frac{1}{12}\sqrt{\frac{20}{\sqrt{7}} - 5}$ which corresponds to the transition point of the Ising model, another interesting point on the non-generic critical line is found for $g = h$. This point corresponds to having a vanishing Ising coupling in which case the model reduces to Bernoulli-1/2 site percolation on random triangulations: by (4.15) we find $\rho = 3/2$ and $g = h = \frac{1}{2\sqrt{2}\cdot 3^{3/4}}$. Note that this value is equal to the critical value of g for pure triangulations divided by $\sqrt{2}$ as it should, since the two choices of spin variables at each vertex are equivalently counted by assigning a weight $\sqrt{2}$ per triangle (there are essentially twice as many triangles as vertices in a planar triangulation).

4.3. The $n \rightarrow 0$ limit

Fig. 5 shows the phase diagram obtained by our calculation in the $n \rightarrow 0$ limit. In this limit, the equation for the non-generic critical line reads explicitly, in parametric

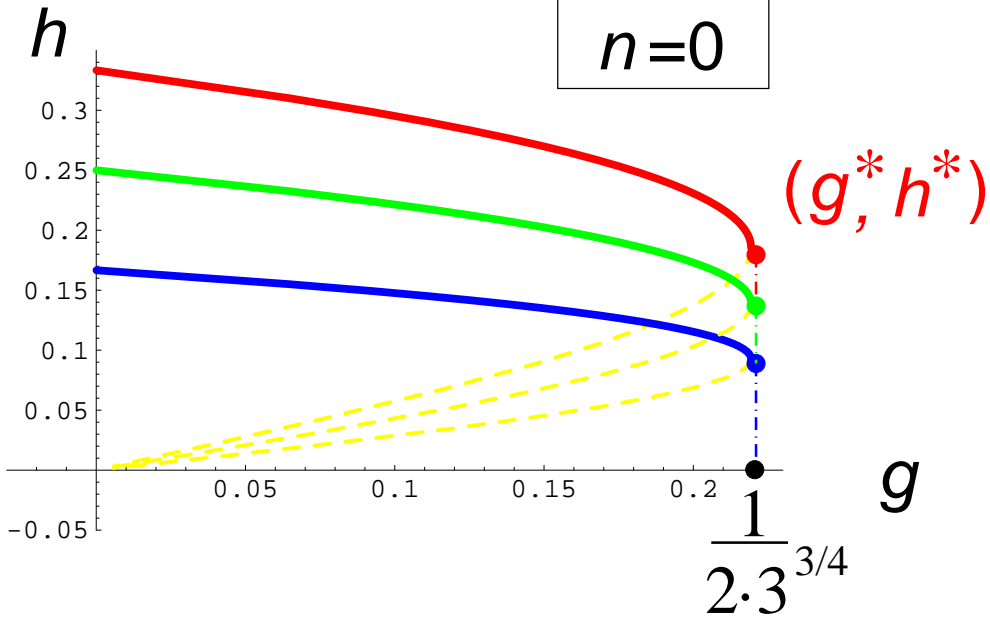


Fig. 5: Exact phase diagram of the $O(n)$ loop model with bending energy in the (g, h) plane, in the limit $n \rightarrow 0$ and, from top to bottom, for $a = 0.5$ (red), 1 (green) and 2 (blue). This phase diagram is similar to that of Fig.3, apart from the fact that the line of non-generic critical points now has an infinite slope at its endpoint (g^*, h^*) . We have $g^* = \frac{1}{2 \cdot 3^{3/4}}$ independently of a , so that the generic critical points now form a vertical segment (dashed line).

form:

$$\frac{g}{h} = \frac{2(a^2 - 1)(c_\infty + 1)(ac_\infty + a - 1)}{2(a - 1)^2 + 4a(a - 1)c_\infty + (2a^2 + 1)c_\infty^2} \quad (4.17)$$

$$h^2 = \frac{-c_\infty^2}{4(a^2 - 1)^2(c_\infty + 1)^2} \frac{2(a - 1)^2 + 4a(a - 1)c_\infty + (2a^2 - 1)c_\infty^2}{2(a - 1)^2 + 4a(a - 1)c_\infty + (2a^2 + 1)c_\infty^2}.$$

The parameter $c_\infty = \cosh v_\infty$ ranges a priori over the real line. By computing discriminants, we observe that the denominator in both fraction is always positive, while the numerator in the expression of h^2 has two real roots at $c_\infty = -2\frac{a-1}{a \pm 1/\sqrt{2}}$. As a consequence, one should reject the values of c_∞ leading to negative values of $\frac{g}{h}$ or h^2 .

The line ends at the dilute point

$$g^* = \frac{1}{2 \cdot 3^{3/4}}, \quad h^* = \frac{1}{(1+a)} \frac{1}{3^{3/4} + 3^{1/4}} \quad (4.18)$$

and, since the value of g^* matches that of the (generic) critical point of pure triangulations, we expect that the generic critical line becomes the vertical segment $\{(g^*, h), 0 \leq h < h^*\}$.

Let us now explain how to recover this phase diagram without recourse to our calculation by the following simple argument. The $n \rightarrow 0$ limit corresponds to configurations of maps with a fixed finite number of loops. The generating function for such configurations may be expressed in terms of the generating function for pure triangulations with a boundary, gathered in the resolvent. For pure triangulations, this resolvent has a cut with endpoints $S \pm 2\sqrt{R}$ where R and S satisfy the relations (see for instance [18])

$$R = 1 + 2gRS, \quad S = g(2R + S^2). \quad (4.19)$$

Now criticality may be achieved in two different ways. The loops may remain small, in which case a generic critical point is simply obtained whenever $dR/dg = \infty$, i.e. $g = g^* = 1/(2 \cdot 3^{3/4})$ irrespectively of h (small enough). We therefore deduce the existence of a vertical line of generic critical points in the (g, h) plane at $g = g^*$. On the other hand, non-generic criticality occurs when the loops become large. Now a loop with contours of lengths k and k' yields a contribution of order $F_k^{\text{pure tri}} F_{k'}^{\text{pure tri}} A_{k,k'}$ to the partition function. In particular, loops of length K (i.e. with $k+k' = K$) contribute at large K as

$$(S + 2\sqrt{R})^K \sum_{k+k'=K} A_{k,k'} \simeq (S + 2\sqrt{R})^K ((a+1)h)^K \quad (4.20)$$

(the reader may easily derive the identity $\sum_{k+k'=K} A_{k,k'} = (x_+^{-K} + x_-^{-K})/2$ where $x_{\pm} = 1/((a \pm 1)h)$ are the fixed points of the involution). The condition for the occurrence of large loops reproduces precisely the non-generic critical condition (4.1), namely

$$\gamma_+ = \frac{1}{(a+1)h} = S + 2\sqrt{R}. \quad (4.21)$$

Using (4.19), this leads immediately to the following parametric form of the non-generic critical line:

$$\begin{aligned} \frac{g}{h} &= (1+a) \left(\sqrt{2\sigma(1-\sigma)} + \sigma \right) \\ g^2 &= \frac{\sigma(1-\sigma)(1-2\sigma)}{2} \end{aligned} \quad (4.22)$$

where we have set $\sigma = gS$ (this parametrization has been introduced in [18]). The value of the parameter σ varies along the line between 0 and $\sigma^* = (3 - \sqrt{3})/6$, corresponding to the dilute point (4.18), which is also the endpoint of the vertical line of generic critical points. Now it is a straightforward exercise to check that the parametrizations (4.17) and (4.22) are indeed fully equivalent upon relating the varying parameters σ and c_{∞} through

$$\sigma = \frac{2(ac_{\infty} + a - 1)^2}{2(a-1)^2 + 4a(a-1)c_{\infty} + (2a^2 + 1)c_{\infty}^2}. \quad (4.23)$$

5. The twisting loop model on quartic maps

The analysis of Section 4 can be applied to obtain the non-generic critical line of the twisting loop model defined in Section 2. To be explicit, we decide to set $g_k^{(0)} = g\delta_{k,4}$, i.e. the faces not visited by the loops are themselves squares, weighted by g . Eq. (2.26) reduces in this case to

$$\tilde{W}(X + i0) + \tilde{W}(X - i0) = 1 - gX - 2n\tilde{W}(h_2^{-1} - X), \quad (5.1)$$

of which we look for a solution $\tilde{W}(X)$ having a cut along the real segment $[0, \Gamma]$ for some positive Γ (recall that the resolvent $W(x)$ is recovered via $W(x) = x\tilde{W}(x^2)$ and has a cut along the real segment $[\gamma_-, \gamma_+]$, with $\gamma_{\pm} = \pm\sqrt{\Gamma}$). Equation (5.1) is similar to (yet even simpler than) (3.7) and we may solve it by the strategy of Section 3.3. It now involves the particular involution $X \mapsto s(X) = h_2^{-1} - X$, here n is replaced by $2n$ and the polynomial V'_0 reads $\tilde{V}'_0(X) = 1 - gX$. As before, we write $\tilde{W}(X) = \tilde{W}_{\text{part}}(X) + \tilde{W}_{\text{hom}}(X)$, with the particular solution (with no cut)

$$\tilde{W}_{\text{part}}(X) = \frac{(1 - gX) - n(1 - g(h_2^{-1} - X))}{2(1 - n^2)} \quad (5.2)$$

and where $\tilde{W}_{\text{hom}}(X)$ is now a solution of the homogeneous equation

$$\tilde{W}_{\text{hom}}(X + i0) + \tilde{W}_{\text{hom}}(X - i0) + 2n\tilde{W}_{\text{hom}}(h_2^{-1} - X) = 0. \quad (5.3)$$

Again, among all solutions of this equation, $\tilde{W}_{\text{hom}}(X)$ is determined by requiring that $\tilde{W}(X)$ has no poles at finite values of X and that $\tilde{W}(X) \sim 1/X$ for $X \rightarrow \infty$. We are here in a situation where $s(\infty) = \infty$ so that, as for loops on triangulations with $a = 1$, we have a single condition to satisfy, namely

$$\tilde{W}_{\text{hom}}(X) = -\frac{(1 - gX) - n(1 - g(h_2^{-1} - X))}{2(1 - n^2)} + \frac{1}{X} + O\left(\frac{1}{X^2}\right). \quad (5.4)$$

The general solution of (5.3) is still given by elliptic functions. Note however that in the elliptic integral (3.17), γ_+ and γ_- should be respectively replaced by Γ and 0. We again concentrate on the non-generic critical case which occurs whenever the endpoint Γ of the cut is a fixed point of the involution $s(X)$, namely $\Gamma = 1/(2h_2)$. The parametrization (3.27) is here replaced by

$$X(v) = \frac{1}{2h_2} \left(1 + \frac{1}{\cosh v} \right). \quad (5.5)$$

Defining

$$\tilde{\omega}(v) = X'(v)\tilde{W}_{\text{hom}}(X(v)) \quad (5.6)$$

as in (3.19), we find that $\tilde{\omega}(v)$ is an odd meromorphic function satisfying the functional equation

$$\tilde{\omega}(v + i\pi) + \tilde{\omega}(v - i\pi) - 2n\tilde{\omega}(v) = 0, \quad (5.7)$$

while Eq. (5.4) translates into

$$\tilde{\omega}(v) = \frac{g}{8h_2^2(1-n)} \frac{1}{(v - \frac{i\pi}{2})^3} + \frac{i(g-2h_2)}{8h_2^2(1+n)} \frac{1}{(v - \frac{i\pi}{2})^2} - \frac{1}{v - \frac{i\pi}{2}} + O(1). \quad (5.8)$$

Again, $\tilde{\omega}(v)$ may be expressed in terms of the fundamental solution ζ of Eq. (3.28), but now with b given by

$$\pi b = \arccos n \quad (5.9)$$

which lies in the range $0 < b < 1/2$ for $0 < n < 1$. We get explicitly

$$\begin{aligned} \tilde{\omega}(v) = & \frac{g}{16h_2^2(1-n^2)} \left(\zeta'' \left(v - \frac{i\pi}{2} \right) - \zeta'' \left(-v - \frac{i\pi}{2} \right) \right) \\ & - \frac{i(g-2h_2)}{8h_2^2(1-n^2)} \left(\zeta' \left(v - \frac{i\pi}{2} \right) - \zeta' \left(-v - \frac{i\pi}{2} \right) \right) \\ & - \frac{1}{1+n} \left(\zeta \left(v - \frac{i\pi}{2} \right) - \zeta \left(-v - \frac{i\pi}{2} \right) \right). \end{aligned} \quad (5.10)$$

Since $W(x) = x\tilde{W}(x^2)$, the spectral density is recovered via

$$\rho(x) = \frac{|x|}{2i\pi} \left(\tilde{W}_{\text{hom}}(x^2 + i0) - \tilde{W}_{\text{hom}}(x^2 - i0) \right) \quad (5.11)$$

so that

$$\rho \left(\pm \sqrt{X(v + i\pi)} \right) = \frac{\sqrt{X(v + i\pi)}}{X'(v + i\pi)} \cdot \frac{\tilde{\omega}(v + i\pi) - \tilde{\omega}(v - i\pi)}{2i\pi} \quad (5.12)$$

for real positive v . Contrary to the previous case, we need not have $\tilde{\omega}(i\pi) = 0$, since $\rho(0)$ does not vanish. But we must impose again the condition $\tilde{\omega}(v) = o(e^{-v})$ for $v \rightarrow \infty$ so that $\rho(\gamma_{\pm}) = 0$. By (3.30) and (5.10), we have the expansion

$$\tilde{\omega}(v) = \tilde{\kappa}(b)e^{-bv} + \tilde{\kappa}(2-b)e^{-(2-b)v} + o(e^{-(2-b)v}) \quad (5.13)$$

with

$$\tilde{\kappa}(b) = \frac{(gb^2 + 16h_2^2(n-1)) \cos \frac{\pi b}{2} - 2b(g-2h_2) \sin \frac{\pi b}{2}}{8h_2^2(1-n^2)}. \quad (5.14)$$

The condition $\tilde{\kappa}(b) = 0$ yields

$$g = \frac{4bh_2 - 16\sqrt{1-n^2}h_2^2}{b \left(2 - b\sqrt{\frac{1+n}{1-n}} \right)}. \quad (5.15)$$

Finally, as before, the positivity of F_k requires that $\tilde{\kappa}(2-b) \geq 0$, which yields the condition

$$g \leq \frac{4(2-b)h_2 + 16\sqrt{1-n^2}h_2^2}{(2-b) \left(2 + (2-b)\sqrt{\frac{1+n}{1-n}} \right)}. \quad (5.16)$$

The non-generic critical line therefore ends at the dilute point

$$g^* = \frac{b(2-b)}{4(\sqrt{1-n} + (1-b)\sqrt{1+n})^2},$$

$$h_2^* = \frac{b(2-b)}{8(1-n + (1-b)\sqrt{1-n^2})}.$$
(5.17)

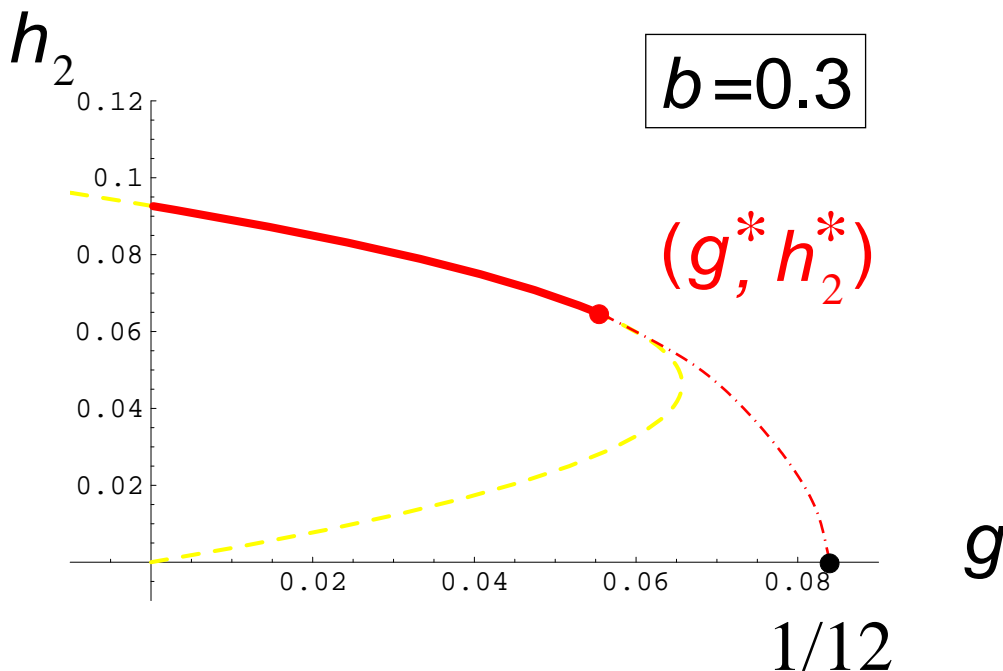


Fig. 6: The phase diagram of the twisting loop model in the variables (g, h_2) for $b = 0.3$ ($n = \cos \pi b$). The line of (dense) non-generic critical points (solid red line) is the portion of the parabola (5.15) (dashed yellow) delimited by the conditions $g \geq 0$ and (5.16). The line ends at the dilute point (g^*, h_2^*) of eq. (5.17). We indicated in dot-dashed line the existence of a line of generic critical points linking the point (g^*, h_2^*) to the point $(1/12, 0)$ describing pure quadrangulations.

The phase diagram of the twisting loop model for $b = 0.3$ is displayed in Fig. 6. A line of generic critical points links the dilute point (g^*, h_2^*) to the critical point of pure quadrangulations without loops at $g = 1/12$, $h_2 = 0$. For illustration, we have also plotted in Fig. 7 the spectral density at the dilute point and at some (arbitrarily chosen) dense point on the non-generic critical line.

When $n \rightarrow 0$, the dilute point (5.17) has coordinates $g^* = 1/12$ and $h_2^* = 1/16$, with the same value of g as for critical pure quadrangulations, so that the generic critical line becomes a vertical segment $\{(1/12, h), 0 < h < 1/16\}$ (see Fig. 8). As for the equation for the the non-generic critical line, it may be recovered by simply writing

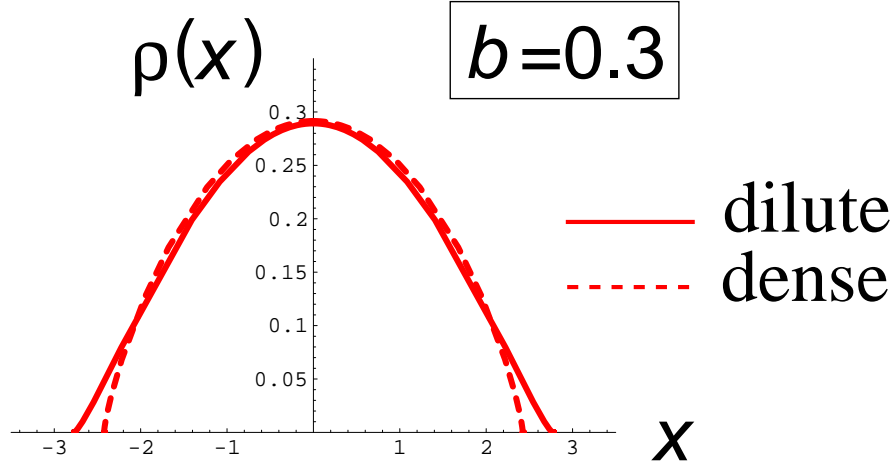


Fig. 7: Plots of the spectral density of the twisting loop model at $b = 0.3$. We plotted the spectral density at the non-generic critical dilute point (g^*, h_2^*) of eq. (5.17) (solid line), and at some (arbitrary) non-generic critical dense point along the non-generic critical line (dashed line).

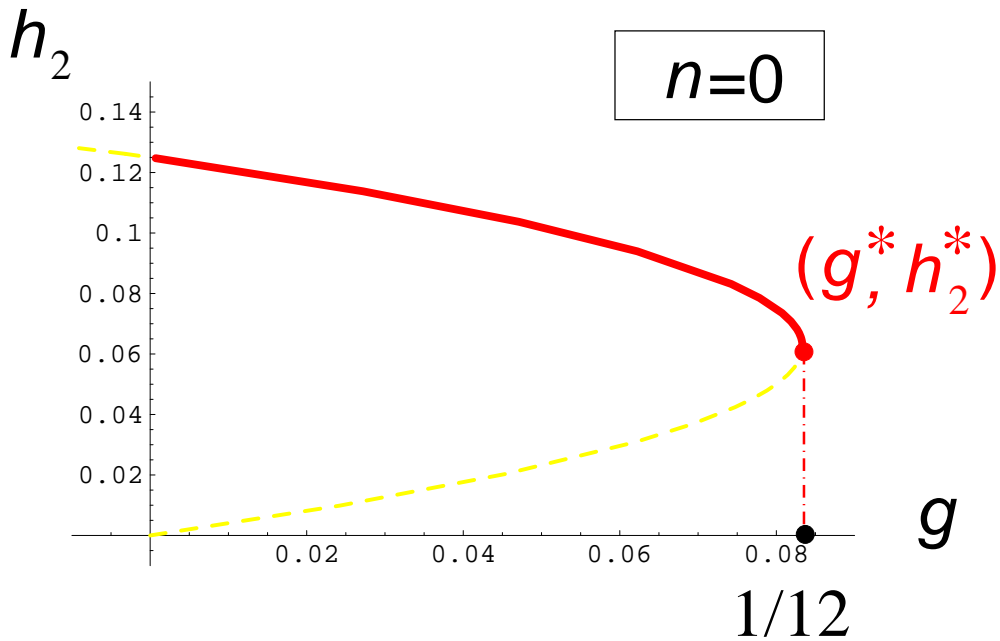


Fig. 8: Phase diagram of the twisting loop model at $n = 0$. The line of non-generic critical points now has an infinite slope at its endpoint (g^*, h_2^*) . We have $g^* = 1/12$ so that the generic critical points now form a vertical segment (dashed line).

that $\Gamma = (\gamma_+)^2$ is the fixed point $1/(2h_2)$ of the involution, with, for $n \rightarrow 0$, a value of γ_+ equal to that of pure quadrangulations. More precisely, we have as in Section 3.5

$\gamma_+ = S + 2\sqrt{R}$, but now with $S = 0$ and R solution of (see for instance [18])

$$R = 1 + 3gR^2 . \quad (5.18)$$

Writing $(2\sqrt{R})^2 = 1/(2h_2)$ leads to

$$g = \frac{8}{3}(h_2 - 8h_2^2) \quad (5.19)$$

which matches (5.15) specialized to $n = 0$, i.e. $b = 1/2$.

6. Analytic properties of the resolvent for maps with controlled face degrees

In this Section, we review a number of analytic properties of the resolvent for maps with controlled face degrees, as we have used them in Section 2 in the framework of our loop models.

6.1. The one-cut lemma for maps with controlled face degrees

We say that a sequence of non-negative numbers $(g_k)_{k \geq 1}$ is *admissible* when the generating function of pointed rooted planar maps with weight g_k per face of degree k is finite. In particular, a model with bounded face degrees corresponds to having all but a finite number of g_k 's non-zero, and such a sequence is admissible when these weights are small enough.

We denote as before by $\mathcal{F}_p(g_1, g_2, \dots)$ the multivariate generating function for maps with a boundary of length p (with the convention $\mathcal{F}_0 = 1$), which is finite whenever the sequence $(g_k)_{k \geq 1}$ is admissible, and we introduce the resolvent

$$\mathcal{W}(x) = \sum_{p \geq 0} \frac{\mathcal{F}_p(g_1, g_2, \dots)}{x^{p+1}} \quad (6.1)$$

(the term resolvent, and the convention of taking $\mathcal{W}(x)$ as a series in $1/x$ are borrowed from random matrix theory). The following property is essential to the determination of $\mathcal{W}(x)$ in specific models:

• **The one-cut lemma:** When $(g_k)_{k \geq 1}$ is an admissible sequence, there exists a real segment $I = [\gamma_-, \gamma_+]$ such that $x \mapsto \mathcal{W}(x)$ defines an analytic function on $\mathbf{C} \setminus I$, which has a finite discontinuity on I . Moreover, we have $|\gamma_-| \leq \gamma_+$ with equality iff $g_l = 0$ for all odd l . Lastly, the spectral density ρ , defined for $x \in I$ by

$$\rho(x) = \frac{\mathcal{W}(x - i0) - \mathcal{W}(x + i0)}{2i\pi} , \quad (6.2)$$

vanishes at the endpoints of I , and is positive in the interior of I .

This lemma essentially follows from the discussion in [19] for the case of a model with bounded face degrees, and we shall extend it to the case of unbounded degrees below. Before, let us review the possible singular behaviours of \mathcal{W} at the dominant singularity γ_+ (γ_- being subdominant except in the bipartite case where \mathcal{W} is odd, hence has the same behaviour at both singularities). For a generic admissible weight sequence, \mathcal{W} has a square-root singularity which, by transfer, corresponds to having $\mathcal{F}_p \sim C \gamma_+^p / p^{3/2}$ for $p \rightarrow \infty$. We say that the model is *non-critical* in this case. Upon increasing the weights up to a point where the sequence is on the verge of becoming non-admissible, we may reach a *critical* point where \mathcal{W} has a higher-order singularity. Generically (for instance, in any model with bounded face degrees), this singularity is of order $(x - \gamma_+)^{3/2}$, in which case $\mathcal{F}_p \sim C \gamma_+^p / p^{5/2}$ and we say, following the terminology of [15], that the model is *generic critical*. However, by suitably fine-tuning all the weights, we may obtain instead a *non-generic critical* model where the singularity is of intermediate order, for instance $(x - \gamma_+)^{\beta}$ with $1/2 < \beta < 3/2$, corresponding to $\mathcal{F}_p \sim C \gamma_+^p / p^{\beta+1}$. These cases encompass all the possible singular behaviours for a non-negative admissible weight sequence.

Our derivation of the one-cut lemma relies on a description of the discontinuity set of \mathcal{W} . We use the relations established in [20] thanks to the bijection between maps and mobiles, and the relation of the latter to Motzkin paths. We need some notations: first, let $\mathcal{F}_p[u]$ (resp. $\mathcal{F}_p^\bullet[u]$) be the generating function of rooted (resp. pointed rooted) maps with root degree p where, on top of the face weights, each vertex of the map is counted with a weight u . Since the two definitions differ only by the marking of a vertex, we have

$$\mathcal{F}_p^\bullet[u] = u \frac{d\mathcal{F}_p[u]}{du}. \quad (6.3)$$

In other words

$$\mathcal{F}_p(g_1, g_2, \dots) = \mathcal{F}_p[u = 1] = \int_0^1 \frac{du}{u} \mathcal{F}_p^\bullet[u]. \quad (6.4)$$

Then, let $P_p(R, S)$ be the generating function of lattice paths in \mathbf{Z}^2 from $(0, 0)$ to $(p, 0)$, where the set of allowed steps consists of:

- level-steps $(i, j) \rightarrow (i + 1, j)$ counted with weight S ;
- up-steps $(i, j) \rightarrow (i + 1, j + 1)$ counted with weight \sqrt{R} ;
- down-steps $(i, j) \rightarrow (i + 1, j - 1)$ also counted with weight \sqrt{R} .

An easy counting argument shows that

$$P_p(R, S) = \sum_{i=0}^{\lfloor p/2 \rfloor} \frac{p!}{(i!)^2 (p - 2i)!} R^i S^{p-2i}. \quad (6.5)$$

We may pack those numbers in the generating function

$$\widehat{P}(x, R, S) = \sum_{p \geq 0} \frac{P_p(R, S)}{x^{p+1}} = \frac{1}{\sqrt{x^2 - 2Sx + S^2 - 4R}}. \quad (6.6)$$

We observe that there exists a segment $\tilde{I}(R, S) = [S - 2\sqrt{R}, S + 2\sqrt{R}]$ such that $x \mapsto \hat{P}(x, R, S)$ is analytic in $\mathbf{C} \setminus \tilde{I}(R, S)$ and has a discontinuity on $\tilde{I}(R, S)$.

The relation established in [20] is that $\mathcal{F}_p^\bullet[u] = u P_p(R[u], S[u])$, where $R[u]$ and $S[u]$ are the unique power series in u and the g_k 's determined by the system

$$\begin{aligned} S[u] &= \sum_{k \geq 1} g_k P_{k-1}(R[u], S[u]) \\ R[u] &= u - \frac{S^2[u]}{2} + \frac{1}{2} \sum_{k \geq 1} g_k P_k(R[u], S[u]) . \end{aligned} \quad (6.7)$$

Actually, $R[u]$ and $S[u]$ have themselves combinatorial interpretations in terms of maps, and $2R[u] + S^2[u]$ is the generating function for pointed rooted maps. In particular, whenever the sequence $(g_k)_{k \geq 1}$ is admissible, $R[u]$ and $S[u]$ are continuous increasing functions of $u \in [0, 1]$, satisfying $R[0] = S[0] = 0$, and having a positive derivative for $u \in [0, 1[$ (their derivative at $u = 1$ are possibly infinite, which corresponds to a critical case). From (6.1) and (6.4), the resolvent can be written as

$$\mathcal{W}(x) = \int_0^1 \frac{du}{\sqrt{x^2 - 2S[u]x + S^2[u] - 4R[u]}} . \quad (6.8)$$

We deduce that $\mathcal{W}(x)$ is an analytic function outside the discontinuity set

$$I = \bigcup_{u \in [0, 1]} [S[u] - 2\sqrt{R[u]}, S[u] + 2\sqrt{R[u]}} . \quad (6.9)$$

It is clear that $u \mapsto S[u] + 2\sqrt{R[u]}$ is a strictly increasing function of u whose derivative does not vanish. Although it is not obvious, we justify in Section 6.3 that $u \mapsto S[u] - 2\sqrt{R[u]}$ must be strictly decreasing with a non-vanishing derivative. Hence

$$I = [\gamma_-, \gamma_+] \quad (6.10)$$

where

$$\gamma_- = S[1] - 2\sqrt{R[1]}, \quad \gamma_+ = S[1] + 2\sqrt{R[1]} \quad (6.11)$$

In particular, we have $|\gamma_-| \leq \gamma_+$, with equality if and only if $S[1] = 0$. From (6.7), this is equivalent to having $g_l = 0$ for all odd integers l , which means that only faces of even degree are allowed. By (6.8) and by monotonicity of $u \mapsto S[u] \pm 2\sqrt{R[u]}$, the spectral density reads, for $x \in]\gamma_-, \gamma_+[$,

$$\rho(x) = \frac{1}{\pi} \int_{u(x)}^1 \frac{du}{\sqrt{4R[u] - S^2[u] + 2S[u]x - x^2}} \quad (6.12)$$

where $u(x)$ is obtained via $S[u(x)] + 2\sqrt{R[u(x)]} = x$ for $x \geq 0$ and via $S[u(x)] - 2\sqrt{R[u(x)]} = x$ for $x < 0$. Clearly, ρ is positive on $] \gamma_-, \gamma_+[$ and the non-vanishing of $(d/du)(S[u] \pm 2\sqrt{R[u]})$ ensures that ρ is continuous and vanishes as $x \rightarrow \gamma_\pm$, as announced. In addition, when $(d/du)(S[u] + 2\sqrt{R[u]})$ is finite at $u = 1$, we may see from (6.8) that \mathcal{W} develops a square-root singularity at γ_+ , i.e. the model is non-critical. When this derivative is infinite, the model is critical: in particular, generic criticality corresponds to $S[u] + 2\sqrt{R[u]}$ having itself a square-root singularity at $u = 1$.

6.2. Functional relation for maps with controlled face degrees

We now assume that $(g_k)_{k \geq 1}$ is an admissible sequence, so that the one-cut lemma applies. The discontinuity of \mathcal{W} on its cut is related to the spectral density ρ by (6.2) and conversely, \mathcal{W} is the Stieltjes transform of ρ , namely

$$\mathcal{W}(x) = \int_{\gamma_-}^{\gamma_+} \frac{\rho(y)dy}{x-y}, \quad \mathcal{F}_k = \int_{\gamma_-}^{\gamma_+} y^k \rho(y)dy. \quad (6.13)$$

We claim that the resolvent $\mathcal{W}(\xi)$ is characterized by $\mathcal{W}(x) \sim 1/x$ and by

$$\forall x \in]\gamma_-, \gamma_+[\quad \mathcal{W}(x+i0) + \mathcal{W}(x-i0) = V'(x), \quad (6.14)$$

where V is the so-called ‘‘potential’’ defined via

$$V'(x) = x - \sum_{k \geq 1} g_k x^{k-1}. \quad (6.15)$$

In terms of the spectral density, this characterization is equivalent to $\int_I \rho(x)dx = 1$ and

$$\forall x \in]\gamma_-, \gamma_+[\quad \text{p.v.} \int \frac{\rho(y)dy}{x-y} = \frac{V'(x)}{2}. \quad (6.16)$$

In this paragraph, we shall justify this functional relation for general admissible sequences.

Tutte’s recursive decomposition [21] of rooted planar maps allows to write, for any sequence of face weights,

$$\mathcal{F}_m = \sum_{k=0}^{m-2} \mathcal{F}_k \mathcal{F}_{m-2-k} + \sum_{k \geq 1} g_k \mathcal{F}_{m+k-2}. \quad (6.17)$$

If we want to write this relation in terms of the resolvent $\mathcal{W}(x)$, we first need to know the location of the singularities of $V'(x)$ which, at first, only makes sense as a power series in x . From (6.7) and the fact that $S[1]$ and $R[1]$ are finite for admissible sequences, we can deduce a lower bound on the radius of convergence of $V'(x)$. We use the asymptotic behaviour of $P_k(R[1], S[1])$ when $k \rightarrow \infty$, which can be extracted from (6.6) by transfer theorems. Since $|\gamma_-| \leq \gamma_+$, γ_+ is always the dominant singularity of $\widehat{P}(x, R[1], S[1])$ and $P_k(R[1], S[1]) = O(k^{-1/2} \gamma_+^{-k})$ (when $S[1] = 0$, $\gamma_- = -\gamma_+$ and P_k vanishes for odd k but the same estimate holds for even k). Accordingly, the radius of convergence of V' is at least γ_+ . In particular, $x \mapsto V'(x)$ defines a real-analytic function at least on the segment $]\gamma_-, \gamma_+[$. So, we may represent, for any integer $m \geq 1$

$$\begin{aligned} -\delta_{k,2} \mathcal{F}_m + g_k \mathcal{F}_{m+k-2} &= \text{Res}_{\xi \rightarrow \infty} \xi^{m-1} (\delta_{k,2} - g_k) \xi^{k-1} \frac{\mathcal{F}_{m+k-2}}{\xi^{(m+k-2)+1}} \\ &= \text{Res}_{\xi \rightarrow \infty} \xi^{m-1} (\delta_{k,2} - g_k) \xi^{k-1} \mathcal{W}(\xi) \\ &= \frac{1}{2i\pi} \oint_{\mathcal{C}} d\xi \xi^{m-1} (\delta_{k,2} - g_k) \xi^{k-1} \mathcal{W}(\xi) \end{aligned} \quad (6.18)$$

where the contour \mathcal{C} surrounds the cut $[\gamma_-, \gamma_+]$ in positive orientation, and is included in the domain of analyticity of V' . To be precise, if V' happens to have a singularity at $\xi = \gamma_+$, we choose a contour sticking to this point when going around the cut. The same caution might be necessary at $\xi = \gamma_- = -\gamma_+$ in the case of maps with even face degrees. This allows to do the summation over k , namely

$$\sum_{k \geq 1} -\delta_{k,2} \mathcal{F}_m + g_k \mathcal{F}_{m+k-2} = -\frac{1}{2i\pi} \oint_{\mathcal{C}} d\xi \xi^{m-1} V'(\xi) \mathcal{W}(\xi) . \quad (6.19)$$

Now, let us take $x \in \mathbf{C}$ such that $|x| > \gamma_+$, and sum over non-negative integers m the equations (6.17) with a weight x^{-m} . All the series involved are convergent and we obtain

$$\mathcal{W}^2(x) - \frac{1}{2i\pi} \oint_{\mathcal{C}} \frac{d\xi}{x-\xi} V'(\xi) \mathcal{W}(\xi) = 0 . \quad (6.20)$$

This is an equality between functions of x which are analytic in the unbounded connected component of $\mathbf{C} \setminus \mathcal{C}$, so it must be valid for any x in this domain. In particular, we can squeeze \mathcal{C} to stick to the cut I , and compute the discontinuity of the left hand side of (6.20) at a point x interior to I , which should equal zero. We find the desired result

$$\forall x \in]\gamma_-, \gamma_+[\quad \mathcal{W}(x+i0) + \mathcal{W}(x-i0) - V'(x) = 0 . \quad (6.21)$$

When $|\gamma_-| < |\gamma_+|$, this relation also holds at $x = \gamma_-$.

6.3. Edge behaviour of the spectral density

We now justify that $u \mapsto S[u] - 2\sqrt{R[u]}$ is a decreasing function of u with a non-vanishing derivative. We may eliminate the case $S[u] = 0$ (i.e. we assume that at least one g_l for odd l is non-zero) as the property is obvious in this case. Our proof, as presented here, relies on real analysis rather than combinatorics. We introduce the shortcut notations $T[u] = \sqrt{R[u]}$, which is a strictly increasing function of u , and $U(\xi) = \sum_{k \geq 1} g_k \xi^{k-1}$. By the same trick that we used in Section 6.2, the relations (6.7) can be rewritten

$$\begin{aligned} S[u] &= \frac{1}{2i\pi} \oint_{\mathcal{C}} \frac{d\xi U(\xi)}{\sqrt{\xi^2 - 2S[u]\xi + S^2[u] - 4T^2[u]}} , \\ 2T^2[u] + S^2[u] &= 2u + \frac{1}{2i\pi} \oint_{\mathcal{C}} \frac{d\xi \xi U(\xi)}{\sqrt{\xi^2 - 2S[u]\xi + S^2[u] - 4T^2[u]}} . \end{aligned} \quad (6.22)$$

These relations are also well-known, and we have justified them for arbitrary (non-negative) admissible weights.

If we use the change of variable $\xi = S[u] + 2T[u] \cos \varphi$ in the integrals, we find

$$\begin{aligned} S[u] &= \frac{1}{\pi} \int_0^\pi d\varphi U(S[u] + 2T[u] \cos \varphi) , \\ T^2[u] &= u + \left(\frac{1}{\pi} \int_0^\pi d\varphi \cos \varphi U(S[u] + 2T[u] \cos \varphi) \right) T[u] . \end{aligned} \quad (6.23)$$

We then differentiate these relations with respect to u , and use an integration by parts to arrive at

$$\begin{aligned} \dot{S}[u] &= \dot{S}[u] L_0[u] + 2\dot{T}[u] L_1[u] , \\ 2T[u]\dot{T}[u] &= 1 + 2T[u]\dot{T}[u] L_0[u] + T[u]\dot{S}[u] L_1[u] , \end{aligned} \tag{6.24}$$

where we have set

$$\begin{aligned} L_0[u] &= \frac{1}{\pi} \int_0^\pi d\varphi U'(S[u] + 2T[u] \cos \varphi) , \\ L_1[u] &= \frac{1}{\pi} \int_0^\pi d\varphi \cos \varphi U'(S[u] + 2T[u] \cos \varphi) . \end{aligned} \tag{6.25}$$

Eqs. (6.24) could have been obtained alternatively upon differentiating directly (6.7) with respect to u . The quantities $L_0[u]$ and $L_1[u]$ would then be identified as generating functions for paths with height difference 0 or 1 at their endpoints, and with a marked point along the path. As such, $L_0[u]$ and $L_1[u]$ are clearly positive. In our setting, this property follows simply from the expressions

$$\begin{aligned} L_0[u] &= \sum_{m \geq 0} \frac{U^{(2m+1)}(S[u])}{(2m)!} (2T[u])^{2m} \left(\frac{1}{\pi} \int_0^\pi d\varphi \cos^{2m} \varphi \right) , \\ L_1[u] &= \sum_{m \geq 0} \frac{U^{(2m+2)}(S[u])}{(2m+1)!} (2T[u])^{2m+1} \left(\frac{1}{\pi} \int_0^\pi d\varphi \cos^{2m+2} \varphi \right) , \end{aligned} \tag{6.26}$$

with $T[u] > 0$, while all derivatives of $\xi \mapsto U(\xi)$ at $S[u] > 0$ are positive since all the g_k 's are non-negative (here we eliminate the trivial case where only g_1 would be non-vanishing). Combining the relations (6.24) and eliminating $L_0[u]$, we deduce

$$(2\dot{T}[u])^2 - (\dot{S}[u])^2 = \frac{\dot{S}[u]}{T[u] L_1[u]} > 0 . \tag{6.27}$$

Since $S[u]$ and $T[u] = \sqrt{R[u]}$ are strictly increasing functions of u , the claim follows: $\dot{S}[u] - 2\dot{T}[u] < 0$.

6.4. Remark on complex valued face weights

Let us say a word on more general, maybe complex valued face weights. To avoid confusion in this paragraph, we shall denote by \mathcal{R} and \mathcal{S} the power series in g_k satisfying (6.7). We say that a sequence of complex numbers $(g_k)_{k \geq 1}$ is *sub-admissible* if the sequence $(|g_k|)_{k \geq 1}$ is admissible. In this case, $\mathcal{R}[u]$ and $\mathcal{S}[u]$ assume finite values for the sequence $(|g_k|_k)$ and any $u \in [0, 1]$, that we denote $R_M[u]$ and $S_M[u]$. Hence, they also assume finite values that we denote $R[u]$ and $S[u]$ for the sequence $(g_k)_{k \geq 1}$ itself, and we have $|R[u]| \leq R_M[u]$ and $|S[u]| \leq S_M[u]$ for all u . Moreover, the radius of convergence of V' is at least $\gamma_{+,M} = S_M[1] + 2\sqrt{R_M[1]}$. Recalling that $S_M[u] + 2\sqrt{R_M[u]}$ increases

with u , we have $|S[u] \pm 2\sqrt{R[u]}| \leq \gamma_{+,M}$. Thus, the disk of convergence of V' contains the interior of the discontinuity set of $\mathcal{W}(x)$ computed with the weights $(g_k)_{k \geq 1}$. This ensures also for sub-admissible sequences the validity of (6.20). The discontinuity set is now:

$$I = \bigcup_{u \in [0,1]} \{x \in \mathbf{C} \quad (x^2 - 2S[u]x + S^2[u] - 4R[u]) \leq 0\} \quad (6.28)$$

It can be quite complicated, since $R[u]$ and $S[u]$ moves in the complex plane when u increases. Nevertheless, we find:

$$\mathcal{W}(x^+) + \mathcal{W}(x^-) - V'(x) = 0 \quad (6.29)$$

for any point x of I such that $|x| < \gamma_{+,M}$ and such that the intersection of I with a small ball B centered at x is a piecewise \mathcal{C}^1 curve separating B in two connected components B_+ and B_- which both intersect the unbounded component of $\mathbf{C} \setminus I$. x^\pm then denote a sequence of points in B_\pm which converges to x .

7. Conclusion and discussion

In this paper, we have shown how the gasket decomposition, upon relating loop models to models of maps with controlled face degrees, immediately provides a functional equation for the resolvent of the model. We then looked for the largest possible class of models for which this functional equation may be solved by the same techniques that were used to solve earlier models. In this respect, it was crucial that the cut $[\gamma_-, \gamma_+]$ interacts with a single mirror image, which is guaranteed if the ring (grand canonical) generating function has a single pole, in which case a homographic involution naturally enters the game (if the model is symmetric). For non-negative weights, this involution is moreover locally decreasing but the solving technique could easily be extended to deal with increasing homographic involutions. We discuss in Appendix A how a non-generic critical point could emerge in this case.

All the above solvable models (with non-negative weights) can be realized within the framework of a single model of loops with bending energy, or for twofold avatars of such models in bipartite maps (such as the twisting loop model). All those models display the same critical behaviours as those observed in previously solved $O(n)$ models and no new universality class is found. In particular, at non-generic critical points, the critical behaviours are also those of maps with large faces, namely the stable maps of [14].

The problem of finding a resolvent satisfying (2.22) for the quadrangular case with arbitrary h_1 and h_2 is much more involved as the cut now interacts with two mirror cuts (its images by y_+ and y_-). This problem is still open and may lead to new interesting critical phenomena. In all generality, loop models may involve several poles for the ring generating function and new techniques are needed to solve these multi-pole models.

As a more promising issue, it is worth mentioning that the nested loop approach can be generalized to describe Potts model (possibly with defects). This again leads to a

functional equation and it may easily be seen that it now involves a pair of homographies which are reciprocal of one another, rather than a single involution. This problem is under investigation.

Acknowledgments: We thank P. Di Francesco for inspiring discussions, and particularly for pointing out the connection with [17]. The work of G.B. is partly supported by the ANR project GranMa “Grandes Matrices Aléatoires” ANR-08-BLAN-0311-01. J.B. acknowledges the hospitality of Laboratoire d’Informatique Algorithmique: Fondements et Applications (LIAFA) of Université Paris Diderot and CNRS, where part of this work was completed.

Appendix A. Case of a general homographic involution

We have seen that a model with non-negative local weights cannot lead to a homographic involution $s(x)$ which is increasing, or for which $s(0) < 0$. Let us nevertheless consider here the case of an arbitrary homographic involution, namely

$$s(x) = \frac{\alpha - \beta x}{\beta - \delta x}, \quad \alpha, \beta, \delta \in \mathbf{R}. \quad (\text{A.1})$$

Recall that s has real fixed points iff it is locally decreasing over \mathbf{R} , i.e. iff $\beta^2 - \alpha\delta > 0$. Such a general homographic involution may be obtained in loop models for a particular set of real weights. We shall assume here that these weights may be chosen in such a way that the resolvent has one cut only on a segment $I = [\gamma_-, \gamma_+]$ of the real line. This requirement is not an empty condition since the one-cut property is not automatic when the weights are not all positive. Note however that, under this assumption (and provided the weights are real), the spectral density must be positive in the interior of I .

We may distinguish six situations, displayed in Fig.9, depending on the local monotonicity of s and on the relative position of I and $s(I)$. We shall now examine these situations and explain when a non-generic critical behaviour can be reached.

The situation **1**– corresponds to a locally decreasing involution with $s(I) > I$. The non-generic critical behaviour is obtained when γ_+ collides with $s(\gamma_+)$, i.e. is one of the fixed points of s . This case can always be realized in a model with bending energy (see Section 3.2), and we have already studied it in details.

The situation **2**– corresponds to a locally decreasing involution for which $s(I) < I$. The non-generic critical behaviour is obtained when γ_- collides with $s(\gamma_-)$, i.e. is again one of the fixed points of s .

The situation **3**– corresponds again to a locally decreasing involution for which the pole of s belongs to I so that $s(I)$ is split into two semi-infinite intervals. The non-generic critical behaviour is obtained when γ_+ collides with $s(\gamma_+)$, or when γ_- collides with $s(\gamma_-)$, or both. This case also arises in a model with bending energy.

The situation **1**+ (resp. **2**+) corresponds to a locally increasing involution for which $s(I) > I$ (resp. $s(I) < I$) and does not feature any non-generic critical behaviour.

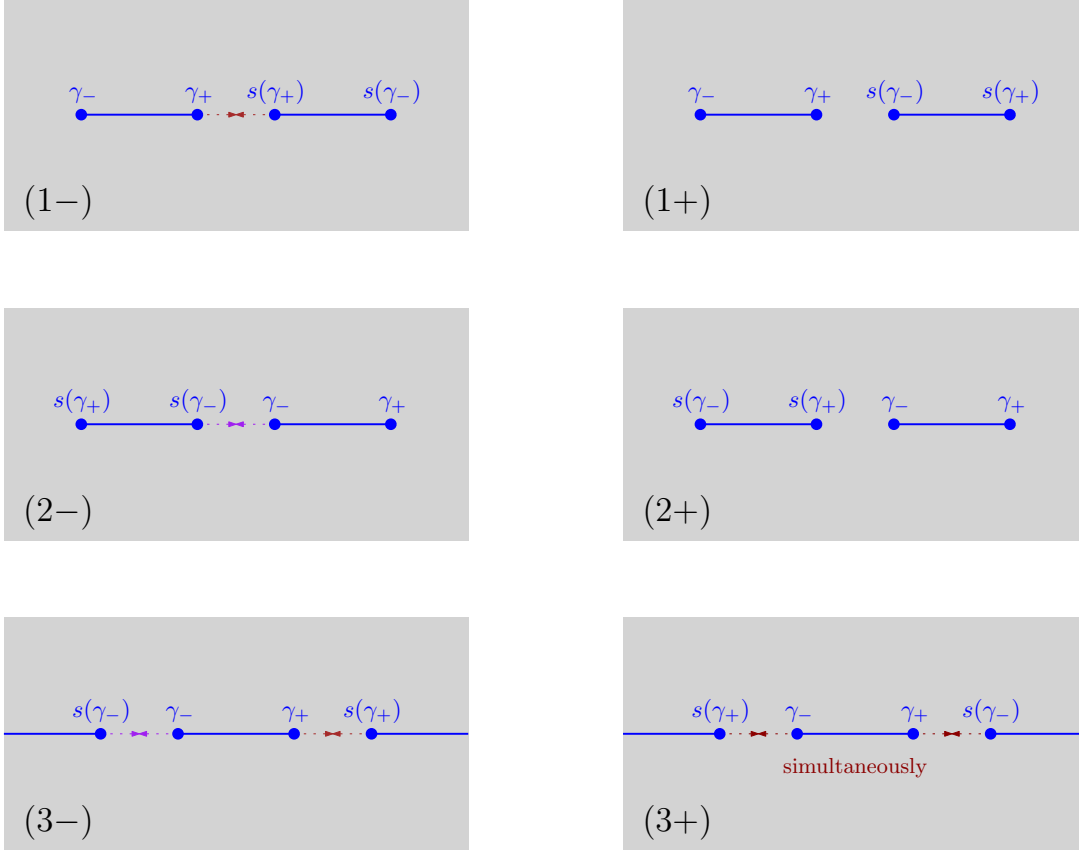


Fig. 9: The six situations for the relative positions of I and $s(I)$ (see text).

Indeed, if γ_{\pm} collides with $s(\gamma_{\mp})$, by involutivity both extremities of I should collide simultaneously with the extremities of $s(I)$, which is clearly not possible.

The situation **3+** corresponds to again to a locally increasing involution for which the pole of s belongs to I , so that $s(I)$ is split into two semi-infinite intervals. A non-generic behaviour is obtained whenever γ_+ collides with $s(\gamma_-)$, which implies that γ_- collides with $s(\gamma_+)$ by involutivity, so that both extremities of I collide simultaneously with the extremities of $s(I)$.

The techniques presented in this article to determine the resolvent $W(x)$ can easily be applied to the six situations. The equations of the critical manifold, and in particular the expression of $W(x)$ on the non-generic critical manifold in terms of trigonometric functions would follow.

References

- [1] W.T. Tutte, *A Census of Planar Maps*, *Canad. J. of Math.* **15** (1963) 249-271.
- [2] See for instance: J.-F. Le Gall and G. Miermont, *Scaling limits of random trees and planar maps*, Lecture notes of the Clay Mathematical Institute Summer School, Buzios (2010), arXiv:1101.4856, and references therein.
- [3] See for instance: P. Di Francesco, P. Ginsparg and J. Zinn–Justin, *2D Gravity and Random Matrices*, *Physics Reports* **254** (1995) 1-131, arXiv:hep-th/9306153, and references therein.
- [4] B. Duplantier and I. Kostov, *Conformal spectra of polymers on a random surface*, *Phys. Rev. Lett.* **61** (1988) 1433-1437.
- [5] I. Kostov, *$O(n)$ vector model on a planar random lattice: spectrum of anomalous dimensions*, *Mod. Phys. Lett.* **4** (1989) 217-226.
- [6] I. Kostov and M. Staudacher, *Multicritical Phases of the $O(n)$ Model on a Random Lattice*, *Nucl. Phys.* **B384** (1992) 459-483, arXiv:hep-th/9203030.
- [7] B. Eynard and J. Zinn–Justin, *The $O(n)$ model on a random surface: critical points and large order behaviour*, *Nucl. Phys.* **B386** (1992) 558-591, arXiv:hep-th/9204082.
- [8] B. Eynard and C. Kristjansen, *Exact solution of the $O(n)$ model on a random lattice*, *Nucl. Phys.* **B455** (1995) 577-618, arXiv:hep-th/9506193.
- [9] B. Eynard and C. Kristjansen, *More on the exact solution of the $O(n)$ model on a random lattice and an investigation of the case $|n| > 2$* , *Nucl. Phys.* **B466** (1996) 463-487, arXiv:hep-th/9512052.
- [10] G. Borot and B. Eynard, *Enumeration of maps with self avoiding loops and the $O(n)$ model on random lattices of all topologies*, *J. Stat. Mech.* (2011) P01010, arXiv:0910.5896.
- [11] V.G. Knizhnik, A.M. Polyakov and A.B. Zamolodchikov, *Fractal Structure of 2D Quantum Gravity*, *Mod. Phys. Lett.* **A3** (1988) 819-826; F. David, *Conformal Field Theories Coupled to 2D Gravity in the Conformal Gauge*, *Mod. Phys. Lett.* **A3** (1988) 1651-1656; J. Distler and H. Kawai, *Conformal Field Theory and 2D Quantum Gravity*, *Nucl. Phys.* **B321** (1989) 509-527.
- [12] G. Miermont, *The Brownian map is the scaling limit of uniform random plane quadrangulations*, arXiv:1104.1606.
- [13] J.-F. Le Gall, *Uniqueness and universality of the Brownian map*, arXiv:1105.4842.
- [14] J.-F. Le Gall and G. Miermont, *Scaling limits of random planar maps with large faces*, *Ann. Probab.* **39(1)** (2011) 1-69, arXiv:0907.3262 [math.PR].
- [15] G. Borot, J. Bouttier and E. Guitter, *A recursive approach to the $O(n)$ model on random maps via nested loops*, *J. Phys. A: Math. Theor.* **45** (2012) 045002, arXiv:math-ph/1106.0153.

- [16] G. Borot, PhD Thesis, Université d'Orsay (2011), available at <http://tel.archives-ouvertes.fr/tel-00625776/en/>.
- [17] P. Di Francesco, E. Guitter and C. Kristjansen, *Integrable 2D Lorentzian Gravity and Random Walks*, Nucl. Phys. **B567** (2000) 515-553, arXiv:hep-th/9907084.
- [18] J. Bouttier, P. Di Francesco and E. Guitter, *Census of planar maps: from the one-matrix model solution to a combinatorial proof*, Nucl. Phys. **B645**[PM] (2002) 477-499, arXiv:cond-mat/0207682.
- [19] M. Bousquet-Mélou and A. Jehanne, *Polynomial equations with one catalytic variable, algebraic series and map enumeration*, J. Combin. Theory Ser. **B 96** (2006) 623-672.
- [20] J. Bouttier and E. Guitter, *Planar maps and continued fractions*, Commun. Math. Phys. **309**(3) (2012) 623-662, arXiv:1007.0419.
- [21] W.T. Tutte, *On the enumeration of planar maps*, Bull. Amer. Math. Soc. **74** (1968) 64-74.